

**SILVER SURFACE ENRICHMENT ON ZSM-5 ZEOLITES FOR THE
CATALYTIC CRACKING OF *n*-PENTANE TO PRODUCE LIGHT OLEFINS**

Warisara Angguravanich

A Thesis Submitted in Partial Fulfillment of the Requirements
for the Degree of Master of Science
The Petroleum and Petrochemical College, Chulalongkorn University
in Academic Partnership with
The University of Michigan, The University of Oklahoma,
and Case Western Reserve University

2021



CU iThesis 6271012063 thesis / recv: 09092564 02:41:52 / seq: 101
1518776057



1518776057

Silver Surface Enrichment on ZSM-5 Zeolites for the Catalytic Cracking of *n*-Pentane to Produce Light Olefins

Miss Warisara Angguravanich

A Thesis Submitted in Partial Fulfillment of the Requirements
for the Degree of Master of Science in Petrochemical Technology
Common Course
The Petroleum and Petrochemical College
Chulalongkorn University
Academic Year 2020
Copyright of Chulabngkorn University

1518776057
CD IThesis 6271012063 thesis / recv: 09092564 02:41:52 / seq: 101

การเสริมพื้นผิวของซีโอไลต์แซคเคสเอ็มไฟว์ด้วยซิลเวอร์สำหรับการแตกตัวด้วยตัวเร่งปฏิกิริยา
ของสารนอร์มัลเพนเทนเพื่อผลิตโอเลฟินส์เบา

น.ส.วริศรา อังกระวนิช

วิทยานิพนธ์นี้เป็นส่วนหนึ่งของการศึกษาตามหลักสูตรปริญญาวิทยาศาสตรมหาบัณฑิต
สาขาวิชาเทคโนโลยีปิโตรเคมี ไม่สังกัดภาควิชา/เทียบเท่า
วิทยาลัยปิโตรเลียมและปิโตรเคมี จุฬาลงกรณ์มหาวิทยาลัย
ปีการศึกษา 2563
ลิขสิทธิ์ของจุฬาลงกรณ์มหาวิทยาลัย

Thesis Title Silver Surface Enrichment on ZSM-5 Zeolites for the
Catalytic Cracking of *n*-Pentane to Produce Light
Olefins
By Miss Warisara Angguravanich
Field of Study Petrochemical Technology
Thesis Advisor Associate Professor SIRIPORN JONGPATIWUT,
Ph.D.

Accepted by The Petroleum and Petrochemical College, Chulalongkorn
University in Partial Fulfillment of the Requirement for the Master of Science

..... Dean of The Petroleum and
Petrochemical College
(Professor PRAMOCH RANGSUNVIGIT, Ph.D.)

THESIS COMMITTEE

..... Chairman
(Professor BOONYARACH KITIYANAN, Ph.D.)

..... Thesis Advisor
(Associate Professor SIRIPORN JONGPATIWUT,
Ph.D.)

..... External Examiner
(Assistant Professor Bussarin Ksapabutr, Ph.D.)

วริศรา อังกระวนิช : การเสริมพื้นผิวของซีโอไลต์แซคอสเอ็มไพร์ด้วยซิลเวอร์สำหรับการแตกตัวด้วยตัวเร่ง
 ปฏิกิริยาของสารนอร์มัลเพนเทนเพื่อผลิตโอเลฟินส์เบา. (Silver Surface Enrichment on ZSM-
 5 Zeolites for the Catalytic Cracking of *n*-Pentane to Produce Light
 Olefins) อ.ที่ปรึกษาหลัก : รศ. ดร.ศิริพร จงผาคิวติ

ผลของการกระจายตัวของซิลเวอร์ส่งผลต่อประสิทธิภาพการเร่งปฏิกิริยาของซีโอไลต์แซคอสเอ็มไพร์ เนื่องจากการบรรจุโลหะซิลเวอร์ในตัวเร่งปฏิกิริยาสามารถส่งเสริมการผลิตของโอเลฟินส์เบาและเพิ่มประสิทธิภาพกระบวนการแตกตัวด้วยตัวเร่งปฏิกิริยาของสารนอร์มัลเพนเทน อย่างไรก็ตามซีโอไลต์แซคอสเอ็มไพร์ที่บรรจุโลหะซิลเวอร์เสื่อมสภาพอย่างรวดเร็วในกระบวนการแตกตัวด้วยตัวเร่งปฏิกิริยาของสารนอร์มัลเพนเทน ดังนั้นการปรับปรุงตัวเร่งปฏิกิริยาดังกล่าวด้วยวิธีการตกเคลือบด้วยของเหลวเคมี (Chemical liquid deposition) และการซัลเฟชัน (Sulfation) จึงถูกนำมาใช้ปรับปรุงประสิทธิภาพการเร่งปฏิกิริยาและเสถียรภาพของซีโอไลต์แซคอสเอ็มไพร์ ซีโอไลต์แซคอสเอ็มไพร์ที่บรรจุโลหะซิลเวอร์ถูกเตรียมโดยวิธีฝังตัวแบบแห้ง (Incipient wetness impregnation) การตกเคลือบด้วยของเหลวเคมี และการซัลเฟชัน ผลการทำงานและเสถียรภาพของตัวเร่งปฏิกิริยาจะได้รับการประเมินและเปรียบเทียบโดยใช้ปฏิกิริยาการแตกตัวด้วยตัวเร่งปฏิกิริยาของสารนอร์มัลเพนเทน เทคนิคการวิเคราะห์คุณลักษณะของตัวเร่งปฏิกิริยาที่เตรียมได้ ได้แก่ เครื่องวิเคราะห์การเลี้ยวเบนรังสีเอกซ์ (XRD) กล้องจุลทรรศน์แบบส่องผ่าน (TEM) เครื่องวิเคราะห์พื้นที่ผิวด้วยเทคนิคบรูนเนอร์-เอมเมทท์-เทลเลอร์ (BET) เครื่องวิเคราะห์ธาตุด้วยเทคนิคเรืองรังสีเอกซ์ (XRF) และเครื่องวิเคราะห์พื้นผิวด้วยเทคนิคโฟโตอิเล็กตรอน (XPS) จากการวิเคราะห์คุณลักษณะของตัวเร่งปฏิกิริยาขึ้นย่นว่า โครงสร้างลักษณะเฉพาะของซีโอไลต์แซคอสเอ็มไพร์ยังคงสภาพอยู่หลังจากปรับปรุงตัวเร่งปฏิกิริยาดังกล่าวด้วยวิธีการฝังตัวแบบแห้ง การตกเคลือบด้วยของเหลวเคมี และการซัลเฟชัน วิธีการตกเคลือบด้วยของเหลวเคมีนั้นบรรจุโลหะซิลเวอร์บนพื้นผิวภายนอกโดยการสร้างชั้นเคลือบที่มีรูพรุนบนพื้นผิวภายนอก นอกจากนี้การซัลเฟชันยังสร้างชั้นของซัลเฟตบนพื้นผิวของชั้นเคลือบที่มีรูพรุน และส่งเสริมกระบวนการแพร่ของสารนอร์มัลเพนเทนในซีโอไลต์แซคอสเอ็มไพร์ ดังนั้นซีโอไลต์แซคอสเอ็มไพร์ที่ถูกปรับปรุงด้วยวิธีการตกเคลือบด้วยของเหลวเคมีและการซัลเฟชันมีประสิทธิภาพการเร่งปฏิกิริยาที่ดีขึ้น และเพิ่มการผลิตโอเลฟินส์เบา รวมถึงมีเสถียรภาพที่ดีในกระบวนการแตกตัวด้วยตัวเร่งปฏิกิริยาของสารนอร์มัลเพนเทน

สาขาวิชา เทคโนโลยีปิโตรเคมี
 ปีการศึกษา 2563

ลายมือชื่อนิสิต
 ลายมือชื่อ อ.ที่ปรึกษาหลัก

6271012063 : MAJOR PETROCHEMICAL TECHNOLOGY

KEYWORD: HZSM-5, Ag-incorporation, Catalytic cracking, Light olefins

Warisara Angguravanich : Silver Surface Enrichment on ZSM-5 Zeolites for the Catalytic Cracking of *n*-Pentane to Produce Light Olefins.
Advisor: Assoc. Prof. SIRIPORN JONGPATIWUT, Ph.D.

The effects of Ag-incorporation on the catalytic performance of ZSM-5 zeolites have been investigated. Since Ag-incorporation can promote the formation of light olefins and significantly enhance catalytic performance in *n*-pentane catalytic cracking. However, the Ag-incorporated ZSM-5 zeolite was rapidly deactivated in *n*-pentane catalytic cracking. Thus, CLD and sulfation methods were introduced to improve catalytic activity and stability of Ag-incorporated ZSM-5 zeolites. The Ag-incorporated ZSM-5 zeolites have been prepared by the incipient wetness impregnation and CLD methods. Moreover, the sulfated catalyst was prepared by the sequential CLD and sulfation of commercial HZSM-5 zeolite. The catalytic activity and stability of Ag-incorporated ZSM-5 zeolites have been evaluated and compared using *n*-pentane catalytic cracking. The effects of the modification methods on the Ag-incorporated ZSM-5 zeolites have been investigated via the characterizations including XRD, TEM, surface area analyzer (BET), XRF and XPS. The catalyst characterizations confirmed that the characteristic ZSM-5 zeolite structure was well preserved after the Ag-incorporation by impregnation, CLD, and sulfation methods. Compared with the Ag-impregnation, the Ag-CLD method forced the introduced Ag concentrating on the external surface by generating a porous overlayer. In addition, the sulfation treatment further generated a surface sulfate phase over the porous overlayer and promoted the diffusion process of *n*-pentane in the ZSM-5 zeolite. Thus, CLD-Ag-Z5 and S-CLD-Ag-Z5 achieved higher light olefins production, and more efficient to maintain catalytic activity in *n*-pentane catalytic cracking in comparison to the parent HZSM-5 and Ag-Z5.

Field of Study:	Petrochemical Technology	Student's Signature
	
Academic	2020	Advisor's Signature
Year:	

ACKNOWLEDGEMENTS

I would like to express my sincere thanks to my thesis advisor, Assoc. Prof. Siriporn Jongpatiwut for her invaluable help and constant encouragement throughout the course of this research. And this thesis would not have been completed without all the support that I have always received from her.

I would like to thank to Prof. Boonyarach Kitiyanan and Asst. Prof. Bussarin Ksapabutr for being my thesis committees and for giving me the suggestion and encouragement.

I wish to acknowledge TOP-PPC laboratory for catalyst testing facilities.

I am grateful for the partial scholarship and partial funding of the thesis work provided by The Petroleum and Petrochemical College and Center of Excellence on Petrochemical and Materials Technology (PETROMAT).

Moreover, I would like to thank all of my friends in Lab 604, including Somluk Sanorkham and Umbon Boonsard for their friendship and assistance.

Finally, I most gratefully acknowledge my parents for all their support throughout the period of this research.

Warisara Angguravanich

TABLE OF CONTENTS

	Page
ABSTRACT (THAI)	iii
ABSTRACT (ENGLISH)	iv
ACKNOWLEDGEMENTS	v
TABLE OF CONTENTS	vi
LIST OF TABLES	viii
LIST OF FIGURES	ix
CHAPTER 1 INTRODUCTION	1
CHAPTER 2 LITERATURE REVIEW	3
2.1 Light Olefins	4
2.2 Naphtha Feedstock.....	4
2.2.1 <i>n</i> -Pentane	4
2.3 Zeolite	5
2.3.1 Zeolite Materials.....	5
2.3.2 ZSM-5 (MFI) Zeolite Structure.....	6
2.4 Catalytic Cracking of Light Alkanes	7
2.4.1 Possible Reaction Pathways for <i>n</i> -Pentane Cracking Over Zeolites.....	7
2.4.2 Modification of Zeolites	9
CHAPTER 3 EXPERIMENTAL.....	12
3.1 Catalyst Preparation.....	13
3.1.1 Parent HZSM-5	13
3.1.2 Incipient Wetness Impregnation.....	13
3.1.3 Chemical Liquid Deposition (CLD) Method	14
3.1.4 Sulfation Method.....	14
3.2 Catalytic Activity Testing.....	14
3.3 Catalyst Characterization.....	15

3.3.1 X-ray Diffraction (XRD).....	15
3.3.2 Transmission Electron Microscope (TEM).....	16
3.3.3 Surface Area Analyzer (BET).....	16
3.3.4 X-ray Fluorescence Spectroscopy (XRF).....	16
3.3.5 X-ray Photoelectron Spectroscopy (XPS).....	17
CHAPTER 4 RESULTS AND DISCUSSION.....	18
4.1 Catalyst Characterization.....	18
4.1.1 X-ray Diffraction (XRD).....	18
4.1.2 Transmission Electron Microscope (TEM).....	19
4.1.3 Surface Area Analyzer (BET).....	21
4.1.4 Ag-composition of Prepared ZSM-5 Catalysts.....	22
4.2 Catalytic Activity Testing.....	25
4.3 Catalytic Stability.....	29
CHAPTER 5 CONCLUSION AND RECOMMENDATIONS.....	32
5.1 Conclusion.....	32
5.2 Recommendations.....	33
APPENDICES.....	34
Appendix A Graphical Abstract.....	34
Appendix B Hydrocarbon Gas Standard.....	35
Appendix C GC-FID Chromatogram Results.....	36
Appendix D Calculation of Activity Testing.....	43
REFERENCES.....	44
VITA.....	46

LIST OF TABLES

	Page
Table 4.1 The textural properties of prepared ZSM-5 catalysts by incipient wetness impregnation, chemical liquid deposition (CLD), and sulfation methods.....	22
Table 4.2 The Ag-composition of prepared ZSM-5 catalysts.....	23
Table B1 Retention times of the hydrocarbon gas standard.....	35



151876057

CU IThesis 6271012063 thesis / recv: 09092564 02:41:52 / seq: 101

LIST OF FIGURES

	Page
Figure 2.1 Examples of olefins.	4
Figure 2.2 Three-dimensional chemical structure of <i>n</i> -pentane.	5
Figure 2.3 Schematic framework of ZSM-5 type zeolite crystal.....	6
Figure 2.4 Possible side reaction routes during <i>n</i> -pentane cracking over zeolites	8
Figure 3.1 Schematic of the catalyst testing unit.	15
Figure 4.1 XRD patterns of P-Z5, Ag-Z5, CLD-Ag-Z5, and S-CLD-Ag-Z5.....	19
Figure 4.2 TEM images of (a) P-Z5 (b) Ag-Z5 (c) CLD-Ag-Z5 (d) S-CLD-Ag-Z5 (e) The rough surface of S-CLD-Ag-Z5.....	20
Figure 4.3 N ₂ adsorption and desorption isotherms of P-Z5, Ag-Z5, CLD-Ag-Z5 and S-CLD-Ag-Z5.	21
Figure 4.4 Ag _{3d5/2} XPS spectra of (a) Ag-Z5 and (b) CLD-Ag-Z5.	24
Figure 4.5 Conversion of <i>n</i> -pentane, ethylene yield, propylene yield and light olefins yield from P-Z5, Ag-Z5, CLD-Ag-Z5 and S-CLD-Ag-Z5 at 550 °C.....	25
Figure 4.6 Products yield of light olefins and paraffins from P-Z5, Ag-Z5, CLD-Ag-Z5 and S-CLD-Ag-Z5 at 550 °C.....	26
Figure 4.7 Products distribution from P-Z5, Ag-Z5, CLD-Ag-Z5 and S-CLD-Ag-Z5 at 550 °C.	27
Figure 4.8 Ethylene selectivity, propylene selectivity and propylene to ethylene ratio from P-Z5, Ag-Z5, CLD-Ag-Z5 and S-CLD-Ag-Z5 at 550 °C.....	28
Figure 4.9 Conversion of <i>n</i> -pentane from P-Z5, Ag-Z5, CLD-Ag-Z5 and S-CLD-Ag-Z5 at 550 °C as a function of time on stream (TOS).	30
Figure 4.10 Light olefins selectivity from P-Z5, Ag-Z5, CLD-Ag-Z5 and S-CLD-Ag-Z5 at 550 °C as a function of time on stream (TOS).	30

Figure 4.11 Ethylene selectivity from P-Z5, Ag-Z5, CLD-Ag-Z5 and S-CLD-Ag-Z5 at 550 °C as a function of time on stream (TOS).....	31
Figure 4.12 Propylene selectivity from P-Z5, Ag-Z5, CLD-Ag-Z5 and S-CLD-Ag-Z5 at 550 °C as a function of time on stream (TOS).....	31
Figure A1 Graphical Abstract.....	34
Figure C1 GC-FID Chromatogram of HZSM-5 catalyst at TOS 1 h.	36
Figure C2 GC-FID Chromatogram of HZSM-5 catalyst at TOS 2 h.	36
Figure C3 GC-FID Chromatogram of HZSM-5 catalyst at TOS 3 h.	36
Figure C4 GC-FID Chromatogram of HZSM-5 catalyst at TOS 4 h.	37
Figure C5 GC-FID Chromatogram of HZSM-5 catalyst at TOS 5 h.	37
Figure C6 GC-FID Chromatogram of HZSM-5 catalyst at TOS 6 h.	37
Figure C7 GC-FID Chromatogram of Ag-Z5 catalyst at TOS 1 h.	37
Figure C8 GC-FID Chromatogram of Ag-Z5 catalyst at TOS 2 h.	38
Figure C9 GC-FID Chromatogram of Ag-Z5 catalyst at TOS 3 h.	38
Figure C10 GC-FID Chromatogram of Ag-Z5 catalyst at TOS 4 h.	38
Figure C11 GC-FID Chromatogram of Ag-Z5 catalyst at TOS 5 h.	38
Figure C12 GC-FID Chromatogram of Ag-Z5 catalyst at TOS 6 h.	39
Figure C13 GC-FID Chromatogram of CLD-Ag-Z5 catalyst at TOS 1 h.....	39
Figure C14 GC-FID Chromatogram of CLD-Ag-Z5 catalyst at TOS 2 h.....	39
Figure C15 GC-FID Chromatogram of CLD-Ag-Z5 catalyst at TOS 3 h.....	39
Figure C16 GC-FID Chromatogram of CLD-Ag-Z5 catalyst at TOS 4 h.....	40
Figure C17 GC-FID Chromatogram of CLD-Ag-Z5 catalyst at TOS 5 h.....	40
Figure C18 GC-FID Chromatogram of CLD-Ag-Z5 catalyst at TOS 6 h.....	40
Figure C19 GC-FID Chromatogram of S-CLD-Ag-Z5 catalyst at TOS 1 h.	40
Figure C20 GC-FID Chromatogram of S-CLD-Ag-Z5 catalyst at TOS 2 h.	41

Figure C21 GC-FID Chromatogram of S-CLD-Ag-Z5 catalyst at TOS 3 h.	41
Figure C22 GC-FID Chromatogram of S-CLD-Ag-Z5 catalyst at TOS 4 h.	41
Figure C23 GC-FID Chromatogram of S-CLD-Ag-Z5 catalyst at TOS 5 h.	41
Figure C24 GC-FID Chromatogram of S-CLD-Ag-Z5 catalyst at TOS 6 h.	42



1518776057

CU Theses 6271012063 thesis / recv: 09092564 02:41:52 / seq: 101

CHAPTER 1

INTRODUCTION

The conversion of low value *n*-pentane into more valuable products such as light olefins is important in the petrochemical industry. Light olefins, especially ethylene and propylene, are used as building block materials for many products, including plastics, detergents, and adhesives. Traditionally, naphtha thermal cracking is the main source of light olefins. However, the disadvantages of naphtha thermal cracking are its high process temperature ($>800\text{ }^{\circ}\text{C}$) which results in a massive CO_2 emission, low light olefins yield and propylene to ethylene ratio (Vasudev Pralhad Haribal, 2018). Naphtha catalytic cracking process was more energy-saving and environment-friendly in comparison to thermal cracking. Nowadays, naphtha catalytic cracking has received the worldwide attention. Zeolites with unique structure and acidic properties have exhibited excellent performance in naphtha catalytic cracking, reducing reaction temperature and increasing light olefins production. The high-efficiency zeolite catalysts have been developed in naphtha catalytic cracking technology.

The modified ZSM-5 zeolites can promote the naphtha conversion and light olefins production. Metal-incorporation is a common method to modify ZSM-5 zeolites, and the metals included alkaline earth metal, rare earth metal, transition metal, etc. In addition, the methods for metal-incorporation also improve the catalytic activity and stability of ZSM-5 zeolites. Xu Hou (Hou, Qiu, Zhang, *et al.*, 2017) has studied influences of metal-incorporated HZSM-5 zeolite on reaction pathways for *n*-pentane cracking, including alkaline earth (Sr), rare earth (La), and transition elements (Zr, Ag). The metal-incorporated HZSM-5 zeolite were prepared via the impregnation method. It was found that the Ag-incorporation improved light olefins selectivity that resulted in low value of propylene to ethylene ratio.

One of the most found problems in the *n*-pentane catalytic cracking is coke deposition on active sites of the catalysts that reduces catalyst stability, leading to catalyst deactivation. The addition of metal onto the external surface of ZSM-5 zeolites by the CLD surface modification method was efficient to suppress coke accumulation in *n*-pentane catalytic cracking. Compared with the impregnation method, the CLD

method generated the metal-loading concentrating on the external surface of ZSM-5 zeolites. Xu Hou and his coworkers (Hou *et al.*, 2019) have successfully added ZrO_2 onto the external surface of ZSM-5 zeolites by the CLD strategy. It was found that the surface enrichment of ZrO_2 on ZSM-5 catalysts exhibited higher catalytic activity as well as catalytic stability and decreased the coke formation in *n*-pentane catalytic cracking compared with the parent HZSM-5. The similar results can be expected in the case of sulfated catalyst. Hou and his coworkers (Hou, Qiu, Yuan, Zhang, *et al.*, 2017) have successfully added $\text{SO}_4^{2-}/\text{TiO}_2$ phase onto the external surface of ZSM-5 zeolites via the sequential TiO_2 -CLD and sulfation method. It was found that the $\text{SO}_4^{2-}/\text{TiO}_2/\text{ZSM-5}$ catalysts exhibited excellent catalytic stability and coke resistance ability in normal paraffin cracking. Xu Hou and his coworkers (Hou *et al.*, 2019) have also found that $\text{SO}_4^{2-}/\text{ZrO}_2/\text{ZSM-5}$ achieved the highest light olefins production, which was higher than the Zr-CLD modified and parent HZSM-5.

The purpose of this work is to study the effects of Ag-incorporation on the catalytic performance of ZSM-5 zeolites. the Ag-incorporation was carried out via the impregnation, chemical liquid deposition (CLD) and sulfation methods to obtain the Ag distribution and surface enrichment. The influences of the modification methods on the Ag-incorporated ZSM-5 zeolites were investigated via the catalyst characterizations including XRD, TEM, surface area analyzer (BET), XRF and XPS. The catalytic activity and stability of Ag-incorporated HZSM-5 zeolites were evaluated and compared using *n*-pentane catalytic cracking as a model reaction. In this research, CLD-Ag-Z5 and S-CLD-Ag-Z5 were expected to achieve higher light olefins production, and more efficient to maintain catalytic activity and inhibit coke formation in *n*-pentane catalytic cracking in comparison to the parent HZSM-5 and Ag-impregnated HZSM-5 zeolite.

CHAPTER 2

LITERATURE REVIEW

Light olefins which are in the class of unsaturated hydrocarbons with a single double bond and a chemical formula of C_nH_{2n} are one of the most important chemicals and raw materials in the petrochemical industry. In addition, Light olefins are used as building block materials for many products, including plastics, detergents, and adhesives. Ethylene is the largest volume organic chemical produced globally and a basic building block for the chemistry industry.

The demand for light olefins continues to grow promoting the progress of the global petrochemical market. Ethylene and propylene are the most important olefins. The annual production is about 1.5×10^8 t and 8×10^7 t, respectively (Amghizar *et al.*, 2017). These production rates are expected to increase because of an increasing global population combined with rising living standard. Hence, the light olefins production has become an important measure of economic development. The conventional technologies to produce light olefins are steam cracking, catalytic cracking using zeolites, deep catalytic cracking, and methanol to olefins (MTO).

Traditionally, naphtha thermal cracking process or steam cracking is the main source for light olefins for more than ninety years. This technology has reached to its full capacity and cannot accommodate excessive demands of the petrochemical industry although still 95% of the light olefins are produced by this technology. However, the yield of ethylene and propylene from steam cracking is only 13% and 5% (Yaripour *et al.*, 2015). The feedstock ranges from light alkanes such as ethane and propane to complex mixtures such as naphtha and gas oils that primarily originate from fossil resource. In this process, the hydrocarbon feedstock is mixed with steam and cracked at elevated temperatures in tubular reactors suspended in a gas-fire furnace. Nevertheless, the disadvantages of steam cracking are high energy consumption, massive CO_2 emission, low light olefins yield and propylene to ethylene ratio, etc. An alternative and promising route to produce light olefins which consumes less energy and produces fewer pollutants to the environment is naphtha catalytic cracking process. Zeolite catalysts with unique structure and acidic properties have exhibited excellent



1518776057

CU Theses 6271012063 thesis / recv: 09092564 02:41:52 / seq: 101

activity and stability in naphtha catalytic cracking, reduced reaction temperature and increased light olefins production.

2.1 Light Olefins

Light olefins are unsaturated hydrocarbons containing a single carbon-carbon double bonds, also known as alkenes. The general formula of olefins is C_nH_{2n} ($R-CH=CH-R'$) where n is the number of carbon atoms. Light olefins are not naturally present in crude oils, but they are formed during the conversion processes. These processes include thermal cracking and other catalytic cracking operations. Compared to paraffins, that are saturated hydrocarbons, light olefins are unstable and can reacted themselves or with other compounds such as oxygen and bromine solution. The lightest alkenes are ethylene (C_2H_4) and propylene (C_3H_6), which are important feedstocks for the petrochemical industry.



Figure 2.1 Examples of olefins.

2.2 Naphtha Feedstock

Naphtha is a flammable liquid hydrocarbon mixture and used as solvent and diluent and as raw material for conversion to gasoline. In addition, naphtha is a lightweight petrochemical feedstock that is separated from crude oil in the fractional distillation process along with kerosene and jet fuel.

2.2.1 *n*-Pentane

Pentane, also known as *n*-pentane or $CH_3(CH_2)_3CH_3$, is principally derived from crude oil and is classified as an aliphatic hydrocarbon. It is a colorless, volatile petroleum distillate that is relatively soluble in water and is present as a major component of gasoline.

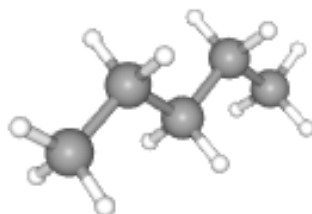


Figure 2.2 Three-dimensional chemical structure of *n*-pentane.

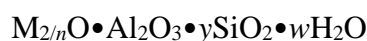
Pentane is relatively inexpensive and is the most volatile alkanes that is liquid at room temperature, so it is often used in the laboratory as solvent that can be conveniently evaporated. However, due to its non-polarity and lack of functionality, it can only dissolve non-polar and alkyl-rich compounds. *n*-pentane is miscible with most common nonpolar solvents such as chlorocarbons, aromatics, and ethers. It is also often used in liquid chromatography.

Pentane is used as a fuel; in the production of ammonia, olefin, and hydrogen; in the manufacture of artificial ice; in low-temperature thermometers; as a blowing agent for plastics and foams; and in solvent extraction processes.

2.3 Zeolite

2.3.1 Zeolite Materials

Zeolite materials are crystalline aluminosilicates of group IA and group IIA elements, such as sodium, potassium, magnesium, and calcium. Chemically, they are represented by the empirical formula:



where y is 2-200, n is the cation valence, and w represents the water contained in the voids of the zeolite.

Zeolites exhibit pore sizes from 0.3 to 1.0 nm and pore volumes from about 0.10 to 0.35 cm³/g. For example, ZSM-5 has medium pore zeolites with 10-ring pores, 0.45-0.60 nm in free diameter.

Zeolites are being widely employed as sorbents, ion exchangers in detergents, or as catalysts for upgrading and/or production of liquid fuels and

intermediates for the petrochemical, chemical, or pharmaceutical industry. Besides their excellent physicochemical properties and high functionality, zeolites have an additional advantage: they are environmentally friendly, safe, and sustainable, and this is a key driving force for green alternatives, for example, chlorine in swimming pools, or to mineral acids, such as hydrochloric, hydrofluoric, or sulfuric acid, in many catalytic industrial processes.

2.3.2 ZSM-5 (MFI) Zeolite Structure

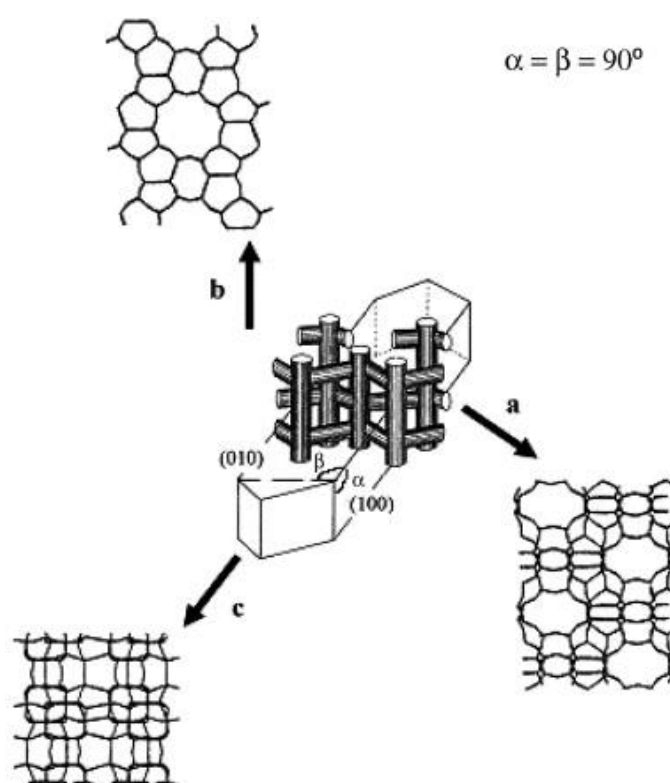


Figure 2.3 Schematic framework of ZSM-5 type zeolite crystal (Yu et al., 2006).

ZSM-5-type zeolites are highly siliceous with Si/Al ratios from about 10 to infinity. Generally, the higher the Si/Al ratio is easier to synthesis. ZSM-5 zeolites are hydrophobic and organophilic solids. Therefore, ZSM-5 zeolites are useful for removing organics from water streams and stable for separations and catalysis in the presence of water.

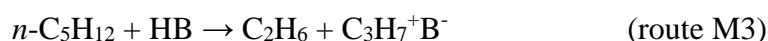
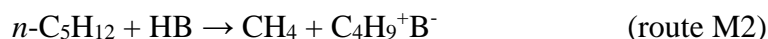
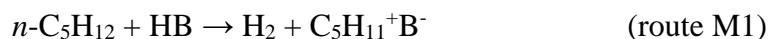
Since ZSM-5 zeolites are highly siliceous the number of cations is small. However, since all the cation sites are in the ZSM-5 channels, all changes to cation number and type can affect the adsorption properties. The adsorption capacity of alkanes in ZSM-5 has been shown to increase with decreasing non-framework cation density (increasing Si/Al ratio) and the linear/branched separation selectivity increases with increasing non-framework cation density. Molecular simulations indicate that for a given cation, the adsorption of alkanes in ZSM-5 increases with decreasing the non-framework cation concentration and, for a given Si/Al ratio, the adsorption of alkanes in ZSM-5 increases with decreasing atomic weight of the non-framework cation.

2.4 Catalytic Cracking of Light Alkanes

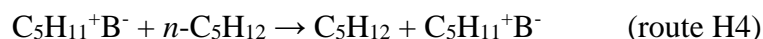
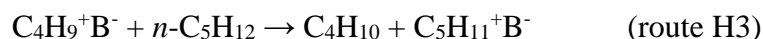
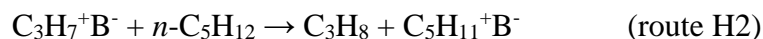
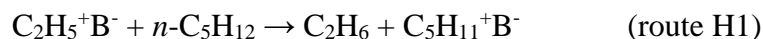
2.4.1 Possible Reaction Pathways for *n*-Pentane Cracking Over Zeolites

The general reaction pathways for *n*-pentane cracking can be described as follows:

- (1) Initial reactions are the monomolecular protolytic cracking of *n*-pentane generating H₂, CH₄, C₂H₆, and C₃H₈ together with carbenium ions of C₅H₁₁⁺, C₄H₉⁺, C₃H₇⁺, and C₂H₅⁺ (routes M1-M4), respectively.



- (2) Hydride transfer reaction would take place between *n*-pentane molecules and the generated carbenium ions giving pentane, butane, propane, ethane, and C₅H₁₁⁺ ions (routes H1-H4), respectively.



- (3) At the same time, β -scission reactions may take place at the specific carbenium ions, such as $C_4H_9^+$ or $C_5H_{11}^+$, generating light olefins and lighter carbenium ions (routes B1-B3).



- (4) For termination step, the deprotonation of carbenium ions gives an olefin and restores acid sites (routes D1-D3).



- (5) In addition, side reactions such as oligomerization, isomerization, cyclization, aromatization, dehydrogenation, etc., may be also involved in the reaction system, enhancing the further conversion and complexity of products (**Figure 2.4**). For example, Oligomerization cracking reaction, etc., promoted the inter-conversion of light olefins.

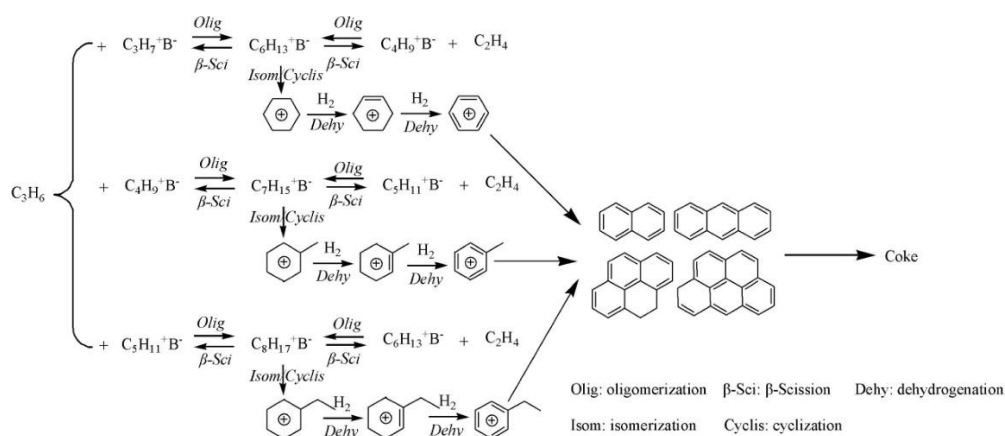


Figure 2.4 Possible side reaction routes during *n*-pentane cracking over zeolites (Hou, Qiu, Zhang, et al., 2017).

The final product distribution in *n*-pentane cracking depends on the relative contribution of reaction pathways.

2.4.2 Modification of Zeolites

The catalytic cracking of various types of hydrocarbons have been investigated over the modified HZSM-5 zeolites to enhance light olefin production. The reaction occurs at 550–650 °C that is about 200 °C lower than steam cracking, and the yields of ethylene and propylene are high enough to compete with the steam cracking products. The effect of feed type on the ratio of light olefins is not as prominent as the steam cracking and the ratios of P/E could be controlled by adjusting the acid type, acid strength, and acid distribution, i.e., Lewis/Brønsted (L/B) acid sites, as well as the operating condition. Thus, high-efficiency zeolite catalysts have been developed in naphtha catalytic cracking.

Influences of zeolite types on product distribution for *n*-pentane cracking over zeolites were explored by Xu Hou and his coworkers (Hou, Qiu, Zhang, *et al.*, 2017). HZSM-5, HZSM-35, and H-Beta were brought to study effects of pore caliber on the reaction pathways and final product distribution in *n*-pentane cracking. Increasing zeolite pore caliber promoted the C-H bond breaking in *n*-pentane cracking. In addition, large zeolite pore caliber and high conversion of *n*-pentane enhanced the hydride transfer and side reactions that were unexpected in paraffin cracking to produce light olefins. Therefore, the decrease of zeolite pore caliber would suppress the C-H bond breaking. Thus, HZSM-5 zeolite with middle pore caliber exhibited the highest selectivity to light olefins in comparison to HZSM-35 and H-Beta.

2.4.1.1 *Metal Incorporation*

The modified ZSM-5 zeolites have been used to promote light olefins production in normal paraffin catalytic cracking. Metal-incorporation is a common method to modify ZSM-5 zeolites, and the metals included alkaline earth metal, rare earth metal, transition metal, etc.

Xu Hou and his coworkers (Hou, Qiu, Zhang, *et al.*, 2017) have been studied Sr, Zr and La-incorporated ZSM-5 zeolites in *n*-pentane catalytic cracking. It was found that the metal-incorporated ZSM-5 zeolites promoted hydride transfer reactions in order of Sr < La < Zr, and the Zr-incorporation helped to promote light olefins production and maintain the catalytic activity while reduced alkenes selectivity.

Due to the excellent catalytic performance of Zr-incorporation, Xu Hou and his coworkers (Hou, Qiu, Yuan, Li, *et al.*, 2017) have been prepared Zr-incorporated HZSM-5 zeolite and Ag-incorporated HZSM-5 zeolite via the impregnation method. It was found that the Zr-incorporation promoted the light olefins yield in naphtha catalytic cracking via hydride transfer. Zr-incorporation enhanced the interaction between the *n*-pentane molecules with Brønsted acid sites or carbenium ions by dispersion forces. However, increasing of hydride transfer reactions promoted the paraffin selectivity such as ethane and propane, with lower the selectivity to hydrogen, methane, and propylene. Although hydride transfer reactions suppressed the side reactions to coke formation. For Ag-incorporation, dehydrogenation cracking over Ag sites significantly promoted C-H bond breaking and alkenes formation i.e., light olefins. Alkenes can be easily protonated by Brønsted acid sites, enhanced conversion of *n*-pentane and thus a higher catalytic activity. On the other hand, Ag-incorporation accelerated the side reactions to coke formation and resulted in a rapid catalyst deactivation.

Therefore, the modification methods also improve the catalytic performance of HZSM-5 zeolites. Chemical liquid deposition (CLD) method is used for external surface modification. It is simple and easy to carry out in a large scale compared with chemical vapor deposition (CVD). Moreover, CLD modification is effective to reduce coke accumulation over ZSM-5 zeolites in normal paraffin catalytic cracking.

Xu Hou and his coworkers (Hou *et al.*, 2016) have been synthesized surface modified catalysts with a silica (SiO₂) or titania (TiO₂) overlayer via the CLD method. It was found that the MFI structure and acid properties of ZSM-5 crystallite were preserved after CLD modification. The CLD method enhanced the sorption process of reactant molecules into the ZSM-5 micropores, and thus promoted the catalytic activity in paraffin cracking. It also was found that the CLD modification suppressed formation of coke on the external surface and/or at the pore mouth.

For sulfation method, the catalyst was prepared by the sequential CLD and sulfation of ZSM-5 zeolites and exhibited excellent performance in normal paraffin catalytic cracking. Xu Hou and his coworkers (Hou, Qiu, Yuan, Zhang, *et al.*, 2017) have been prepared SO₄²⁻/TiO₂/ZSM-5 catalyst. It exhibited excellent activity as

well as stability in normal paraffin catalytic cracking, and thus achieved a higher light olefins production.

Due to the outstanding performance of CLD and sulfation methods to modifying the external surface of ZSM-5 zeolite. Xu Hou (Hou *et al.*, 2019) have been prepared Zr-incorporated ZSM-5 zeolites via the impregnation, chemical liquid deposition (CLD), and sulfation methods. The Zr-CLD modification forced the introduced ZrO₂ concentrating on the external surface and generated a porous overlayer in comparison to the Zr-impregnation. In addition, CLD-Zr-Z5 exhibited an excellent activity and higher light olefins production. Moreover, CLD-Zr-Z5 decreased the coke accumulation in *n*-pentane catalytic cracking compared with the parent HZSM-5. Furthermore, S-CLD-Zr-Z5 exhibited the highest light olefins production, and more efficient to maintain catalytic stability in *n*-pentane catalytic cracking in comparison to P-Z5 and CLD-Zr-Z5.



1518776057

CD IThesis 6271012063 thesis / recv: 09092564 02:41:52 / seq: 101

CHAPTER 3

EXPERIMENTAL

Materials and Equipment

Materials:

Gases

1. High purity hydrogen (HP grade, 99.99% purity) used for FID detector was supplied from Air Liquid, Thailand.
2. High purity nitrogen (HP grade, 99.99% purity) used for purging catalysts after reaction testing and carrier gas was supplied from Air Liquid, Thailand.
3. High purity zero grade air (HP grade, 99.99% purity) used for FID detector was supplied from Air Liquid, Thailand.
4. Ultra-high purity helium (UHP grade, 99.995% purity) used for TCD detector was supplied from Air Liquid, Thailand.

Chemicals

1. *n*-Pentane (C₅H₁₂, 99% purity) was supplied from RCI Labscan, Thailand.
2. Commercial ZSM-5 zeolite (SiO₂/Al₂O₃ ratio of 50) was supplied from Zeolyst, USA.
3. Silver (I) nitrate (AgNO₃, ≥ 99 % purity) was purchased from Sigma Aldrich, USA.
4. Silver (I) sulfate (Ag₂SO₄, 99% purity) was purchased from Sigma Aldrich, USA.
5. Sodium ethoxide (95%) was purchased from Sigma Aldrich, USA.
6. Anhydrous ethanol (C₂H₅OH) was supplied from Merck, Germany.
7. Ammonium sulfate ((NH₄)₂SO₄) was purchased from Ajax Finechem, Australia.

Equipment:

1. Catalytic testing system consisting of feed tank, mass flow controller, back pressure regulator, furnace, and 1/2" O.D. x 19.5" long stainless-steel reactor.
2. Shimadzu GC-2014 gas chromatograph equipped with HP-PLOT/Al₂O₃ and Rtx-1 columns.
3. X-ray diffractometer – XRD (Rigaku)
4. X-ray fluorescence spectrometer – WDXRF (S8-Tiger)
5. Surface analyzer – BET analysis (Quantachrom/Autosorb 1-MP instrument)
6. Transmission electron microscope - TEM (JEM-1400)

Experimental Procedures**3.1 Catalyst Preparation****3.1.1 Parent HZSM-5**

Commercial HZSM-5 zeolite with a SiO₂/Al₂O₃ ratio of 50 was calcined at 550 °C for 5 h and denoted as P-Z5.

3.1.2 Incipient Wetness Impregnation

Silver (I) nitrate (AgNO₃) was dissolved in a designed amount of deionized (DI) water to form the AgNO₃ solution for impregnation. Then, AgNO₃ solution was added in the P-Z5 (3 g) at room temperature. After that, the sample was collected, dried at 120 °C for 4 h, and calcined at 550 °C for 5 h. The modified catalyst was denoted as Ag-Z5.

3.1.3 Chemical Liquid Deposition (CLD) Method

Silver sulfate was brought to react with sodium alkoxide in absolute ethanol for 1 h thus silver alkoxide was completely obtained as a blackish powder. Then, the sample was collected. The silver alkoxide powder was added into the anhydrous ethanol, and a homogeneous solution was achieved by the intense stir. Then, P-Z5 (3 g) was added into the homogeneous solution and stirring for 1 h. The sample was collected by filtration, repeatedly washed with ethanol, dried at 120 °C for 4 h, and calcined at 550 °C for 4 h. The obtained zeolite catalyst was denoted as CLD-Ag-Z5.

3.1.4 Sulfation Method

The obtained CLD-Ag-Z5 (3 g) was brought to react with (NH₄)₂SO₄ solution (1 mol/L, 60 mL) at room temperature under stirring for 8 h (Hou *et al.*, 2019). Then, the sample was collected by filtration, dried at 120 °C for 4 h, and calcined at 550 °C for 3 h. The obtained zeolite catalyst was denoted as S-CLD-Ag-Z5.

3.2 Catalytic Activity Testing

The *n*-pentane cracking test was carried out in a continuous flow fixed-bed reactor. In each test, 2 g of fresh catalyst was packed in a 1/2" O.D. x 19.5" long stainless-steel reactor, the modified catalyst was reduced by hydrogen with flow rate of 150 mL/min at 550 °C for 1 h. Then, *n*-pentane feed was continuously injected by feed tank and preheated to 70 °C with a flow rate of 0.270 mL/min for obtaining WHSV of 5 h⁻¹. Nitrogen was used as a carried gas with a flow rate of 150 mL/min. The reaction was performed at 550 °C under atmospheric pressure. The products were analyzed by a gas chromatograph using a Shimadzu GC-2014 equipped with HP-PLOT/Al₂O₃ and Rtx-1 columns.

The GC column temperature was programmed to obtain an adequate separation of the products. The temperature was first kept constant at 40 °C for 2 minutes, then linearly ramped up to 70 °C with ramp rate 10 °C/min and held for 6 minutes, ramped up to 180 °C with ramp rate 10 °C/min and held for 21 minutes, respectively.

The conversion of feed and selectivity was defined as follows.

$$n\text{-pentane conversion (\%)} = \frac{\text{Weight of feed converted} \times 100 (\%)}{\text{Weight of } n\text{-pentane}}$$

$$\text{Selectivity of product } i (\%) = \frac{\text{Weight of product } i \times 100 (\%)}{\text{Total weight of products}}$$

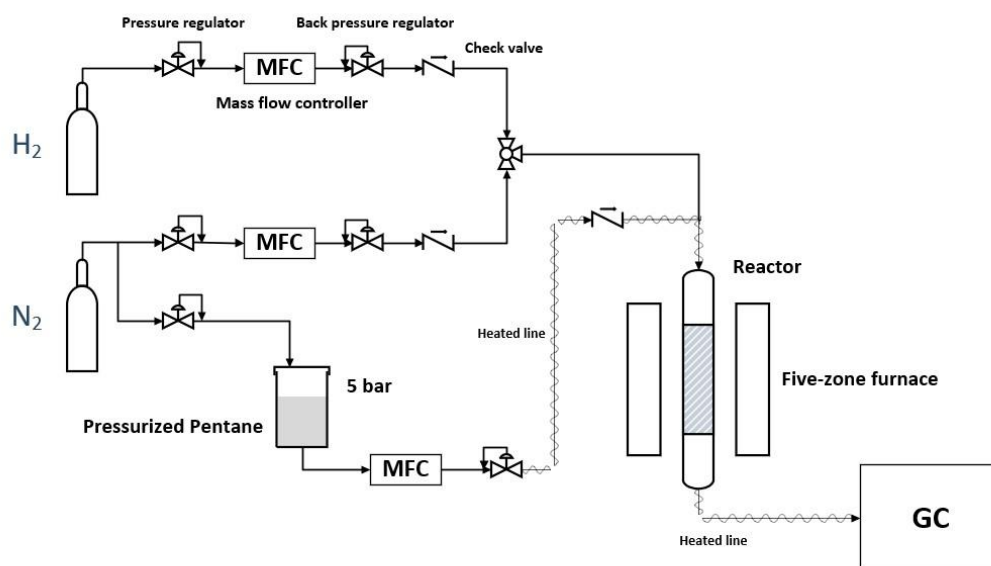


Figure 3.1 Schematic of the catalyst testing unit.

3.3 Catalyst Characterization

3.3.1 X-ray Diffraction (XRD)

X-ray diffraction (XRD) spectroscopy was employed to detect the crystal structure of the catalysts and recorded by a Rigaku X-ray diffractometer. For sample preparation, the sample was ground in mortar and pestle to a fine powder, poured into glass holder and pressed with glass slide. After that, the sample holder was inserted in the XRD instrument. The identification of the ZSM-5 zeolite and modified ZSM-5 was analyzed by a Rigaku X-ray diffractometer with Cu tube for generating CuK α radiation ($\lambda = 1.5418 \text{ \AA}$) at room temperature and operating condition of 40 kV. The sample was measured in the 2θ range of $5\text{-}90^\circ$ with scan speed of $5^\circ/\text{min}$ and scan step size of 0.02° .

3.3.2 Transmission Electron Microscope (TEM)

Transmission electron microscope (TEM) was employed to confirm the existence and distribution of Ag on Ag-incorporated HZSM-5 zeolites and recorded on a transmission electron microscope (JEM-1400). The sample was prepared by the Ultramicrotome Leica EM UC7 for providing ultrathin section as well as smooth surface of the sample. The ultrathin sections of sample collected and moved to a copper grid. Then the sample was coated using a carbon coater which gave ultrathin carbon support film for atomic resolution imaging. After that, the sample was inserted into the TEM instrument. Then the beam of electrons (120 kV) from the electron gun was transmitted through a sample to form a TEM image.

3.3.3 Surface Area Analyzer (BET)

BET analysis was employed to measure surface properties of the catalysts and determined by using Quantachrom/Autosorb 1-MP instrument. In a typical test, the sample was outgassed to remove the humidity and volatile adsorbents adsorbed on surface under vacuum at 300 °C for 12 h prior to the exposure to N₂ at -196 °C. was degassed at 350 °C for 24 h prior to the exposure to N₂ at -196 °C. The specific surface area (S_{BET}) of ZSM-5 zeolites was determined by the Brunauer-Emmett-Teller (BET) method using N₂ adsorption datum. The total pore volume (V_t) was calculated from N₂ uptake at a relative pressure (P/P_0). The micropore surface area (S_{mic}), external surface area (S_{ext}) and micropore volume (V_{mic}) are determined by the t-plot method using N₂ adsorption datum. The mesopore volume (V_{mes}) was calculated by $V_{\text{mes}} = V_t - V_{\text{mic}}$.

3.3.4 X-ray Fluorescence Spectroscopy (XRF)

X-ray fluorescence spectroscopy (XRF) was employed to detect the real percentage of Ag-loading on Ag-incorporated HZSM-5 zeolites and recorded on an X-ray fluorescence spectrometer (WDXRF). For sample preparation, the sample was ground into a fine powder to minimize undesired particle size effects and compressed using a hydraulic press to form a pellet. After that, the sample holder was inserted in the XRF instrument. During the analysis, the sample is irradiated with high energy X-rays from a controlled X-ray tube. When an atom in the sample is struck with an X-ray of sufficient energy (greater than the atom's K or L shell binding energy), an electron

from one of the atom's inner orbital shells is dislodged. The atom regains stability, filling the vacancy left in the inner orbital shell with an electron from one of the atom's higher energy orbital shells. The electron drops to the lower energy state by releasing a fluorescent X-ray. The energy of this X-ray is equal to the specific difference in energy between two quantum states of the electron. The measurement of this energy is the basis of XRF analysis. When X-ray energy causes electrons to transfer in and out of electron orbitals, XRF peaks with varying intensities are created and presented in the spectrum, a graphical representation of X-ray intensity peaks as a function of energy peaks. The peak energy identifies the element, and the peak height or intensity is generally indicative of its concentration.

3.3.5 X-ray Photoelectron Spectroscopy (XPS)

X-ray photoelectron spectroscopy (XPS) was employed to detect the atoms on the external surface of Ag-incorporated HZSM-5 zeolites up to a depth of approximately 10 nm and recorded on a Kratos Axis Ultra DLD. For sample preparation, the sample was dried in the oven, then ground and placed on the carbon tape at the surface of sample bar. After that, the sample bar was inserted into the XPS instrument. The instrument vacuum exceeded 5×10^{-8} Torr during the experiments. The spectra were recorded in constant analyzer energy mode at a pass energy of 140 eV for wide scan mode and 40 eV for narrow scan mode. All spectra were energy calibrated using the internal standard peak (C_{1s}) at the binding energy of 284.7 eV. The data was evaluated using the Vision Processing software, and the background subtraction applied to the high-resolution scans followed the method according to Linear for C_{1s} and Tougaard for Ag_{3d} . Then, the experimental curves were fit for giving deconvolution of XPS spectra. The position and intensity of the peaks in an energy spectrum provide the desired chemical state and quantitative information. The chemical environment of an atom alters the binding energy (BE) of a photoelectron which results in a change in the measured kinetic energy (KE). The BE is related to the measured photoelectron KE by the simple equation; $BE = hv - KE$ where hv is the photon (x-ray) energy. The chemical or bonding information of the element is derived from these chemical shifts.

CHAPTER 4

RESULTS AND DISCUSSION

The purpose of this work is to study the influences of silver distribution, activity, and stability of Ag-Z5, CLD-Ag-Z5 and S-CLD-Ag-Z5 catalysts with different catalyst modification methods on the catalytic cracking of *n*-pentane. The catalysts were investigated via catalyst characterizations including XRD, TEM, surface area analyzer (BET), XRF and XPS.

4.1 Catalyst Characterization

4.1.1 X-ray Diffraction (XRD)

XRD spectra of P-Z5, Ag-Z5, CLD-Ag-Z5 and S-CLD-Ag-Z5 are shown in **Figure 4.1**. The P-Z5 has dominant characteristic diffraction peaks at $2\theta = 7-9^\circ$ and $22-25^\circ$ which examine as the fingerprints of MFI structure and correspond to (1 0 1), (2 0 0), (5 0 1), (1 5 1) and (3 0 3) crystal faces, respectively (Diao *et al.*, 2015). The XRD patterns for Ag-Z5, CLD-Ag-Z5, and S-CLD-Ag-Z5 were similar to that of P-Z5, suggesting that the characteristic MFI structure was preserved after the Ag-incorporation. For metal incorporation and catalyst modification methods, the result could indicate the high dispersion of silver particles on Ag-Z5, CLD-Ag-Z5, and S-CLD-Ag-Z5. Furthermore, there were no additional peaks corresponding to impurities after the surface treatment. This result indicates that catalyst modification methods did not affect the ZSM-5 framework structure.

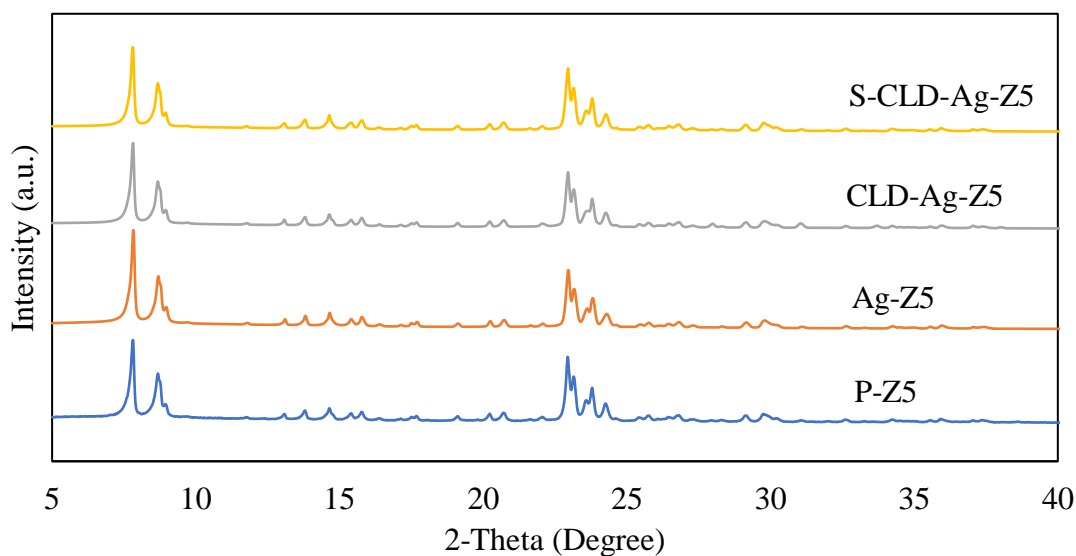


Figure 4.1 XRD patterns of P-Z5, Ag-Z5, CLD-Ag-Z5, and S-CLD-Ag-Z5.

4.1.2 Transmission Electron Microscope (TEM)

TEM analysis was used to confirm the existence and distribution of silver on Ag-incorporated HZSM-5 zeolites. TEM image provided a smooth surface of the P-Z5 at the nano scale. Furthermore, TEM images of the surface of Ag-incorporated HZSM-5 zeolites synthesized via the impregnation, CLD and sulfation methods were also obtained. Ag-incorporation led to the formation of silver particles on Ag-incorporated HZSM-5 zeolites at the nano scale. The silver species mostly distribute on the surface of zeolite particles as silver clusters (Qiu *et al.*, 2014). As shown in **Figure 4.2**, the rough phase of Ag-incorporated HZSM-5 zeolites were rougher than the P-Z5. The rough phase can be attribute to the silver concentrating on the external surface in Ag-incorporated HZSM-5 zeolites. In **Figures 4.2 (c) and 4.2 (d)**, CLD-Ag-Z5 and S-CLD-Ag-Z5 had silver particles aggregation on the support. In **Figure 4.2 (e)**, TEM image of S-CLD-Ag-Z5 showed its rough surface of the sulfate phase on the support (Hou, Qiu, Yuan, Zhang, *et al.*, 2017). In addition, the high dispersion of silver on Ag-incorporated HZSM-5 zeolites was presented in the TEM image. It was consistent with the results of XRD analysis.



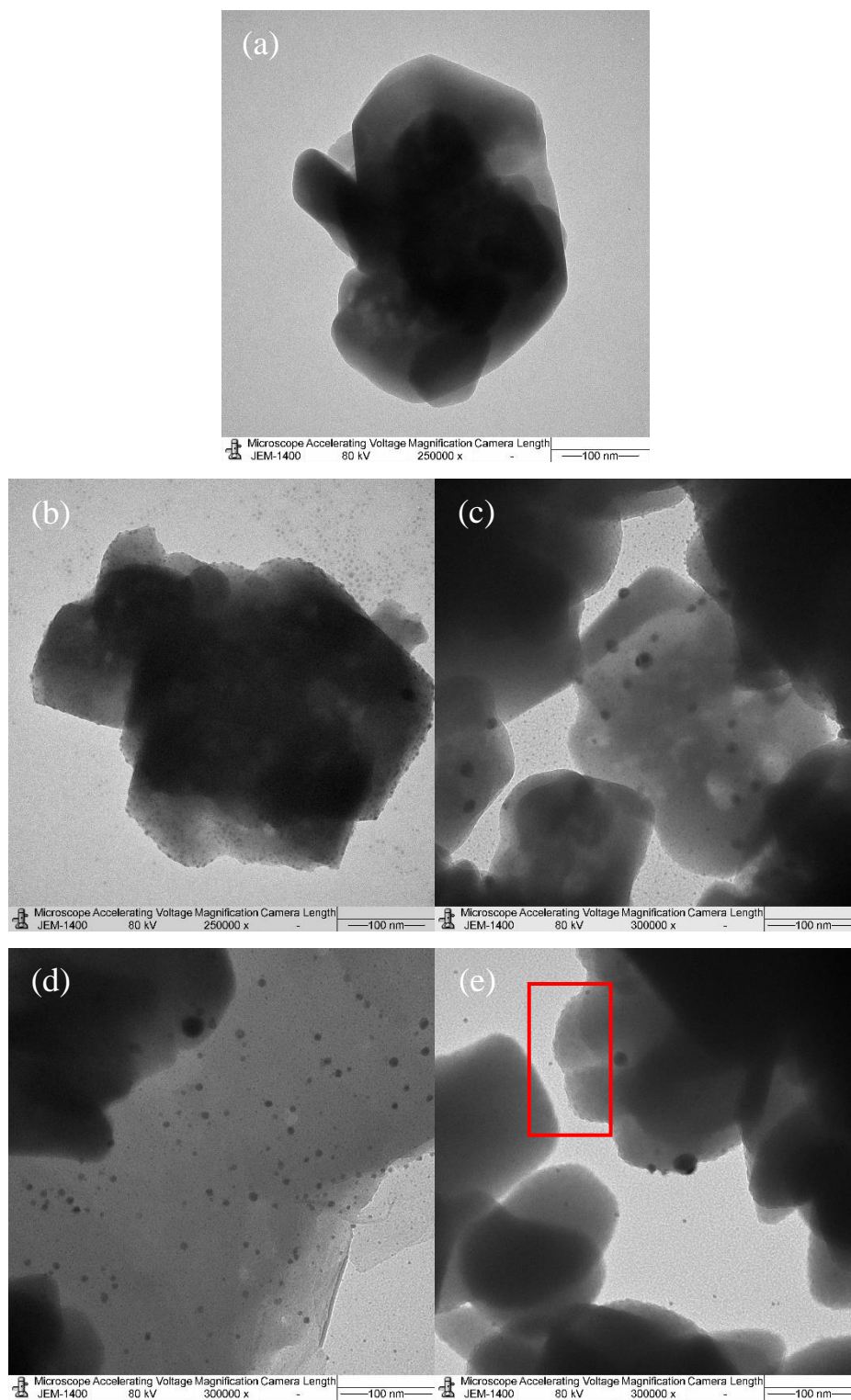


Figure 4.2 TEM images of (a) P-Z5 (b) Ag-Z5 (c) CLD-Ag-Z5 (d) S-CLD-Ag-Z5 (e) The rough surface of S-CLD-Ag-Z5.



151876057

CU IThesis 6271012063 thesis / rev: 09092564 02:41:52 / seq: 101

4.1.3 Surface Area Analyzer (BET)

N_2 adsorption and desorption isotherms were used to characterize the textural properties of the catalysts. As shown in **Figure 4.3**, at low pressure from 0 to 0.2 atm, all the ZSM-5 based catalysts showed an inflection point, which was the characteristic microporous structure of ZSM-5 zeolites and depicted monolayer adsorption. At pressure from 0.3 to 1.0 atm, the type IV isotherms with a hysteresis loop were exhibited in all catalysts indicated the existence of mesoporous structure. It can be attributed to mono-multilayer adsorption of mesoporous adsorbent.

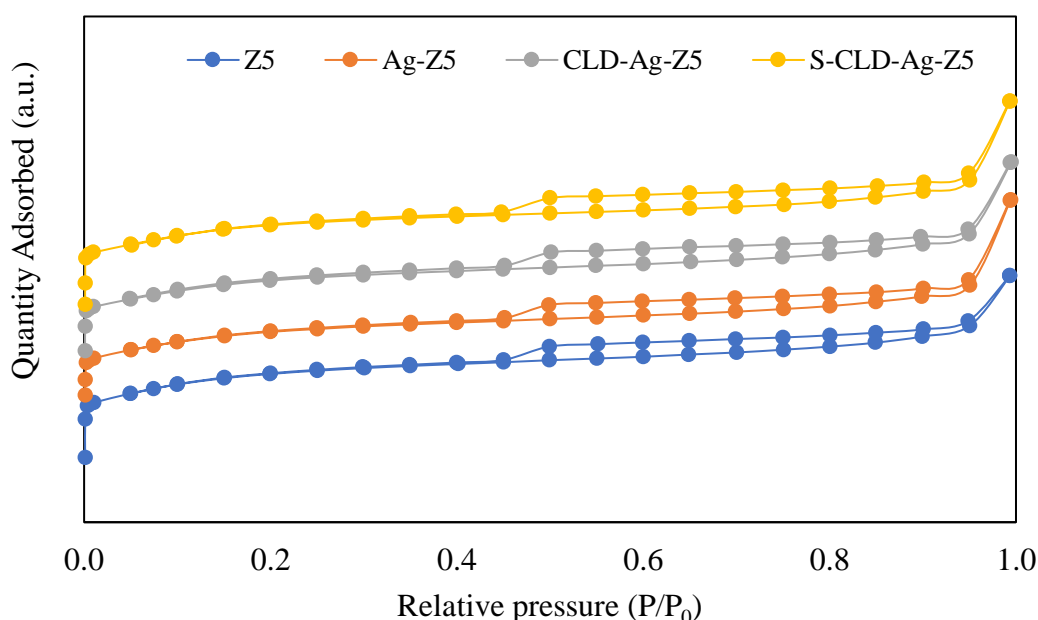


Figure 4.3 N_2 adsorption and desorption isotherms of P-Z5, Ag-Z5, CLD-Ag-Z5 and S-CLD-Ag-Z5.

The textural properties of prepared ZSM-5 catalysts by incipient wetness impregnation, chemical liquid deposition (CLD), and sulfation methods are summarized in **Table 4.1**. The increase of external surface area and mesopore volume of CLD-Ag-Z5 was more significant than that of Ag-Z5, which can be attributed to rough overlayer of silver particles on CLD-Ag-Z5. The overlayer was probably mesoporous phase and expanded the external surface. Furthermore, S-CLD-Ag-Z5 increased total pore volume and mesopore volume. It can be deduced that the sulfation

treatment generated the SO_4^{2-} phase onto the external surface of ZSM-5 and introduced some mesopores into the sulfate phase by the interaction between SO_4^{2-} and silver oxide and increased the surface area. Therefore, S-CLD-Ag-Z5 achieved higher surface area in comparison to Ag-Z5 and CLD-Ag-Z5.

Table 4.1 The textural properties of prepared ZSM-5 catalysts by incipient wetness impregnation, chemical liquid deposition (CLD), and sulfation methods

Catalysts	S_{BET} (m^2/g)	S_{mic} (m^2/g)	S_{ext} (m^2/g)	V_{t} (cm^3/g)	V_{mic} (cm^3/g)	V_{mes} (cm^3/g)
P-Z5	358.7	237.4	121.3	0.302	0.208	0.094
Ag-Z5	338.5	224.2	114.3	0.333	0.172	0.161
CLD-Ag-Z5	330.5	201.5	129.0	0.364	0.168	0.196
S-CLD-Ag-Z5	350.7	235.5	115.2	0.517	0.179	0.338

4.1.4 Ag-composition of Prepared ZSM-5 Catalysts

The real percentage of Ag-composition on Ag-incorporated HZSM-5 zeolites were detected by X-ray fluorescence spectrometer (XRF). As shown in **Table 4.2**, the total Ag-composition on Ag-Z5 and CLD-Ag-Z5 were 0.703, and 0.822 wt%, respectively. Compared with theoretical Ag-loading, the unexpected lower amount of total Ag-composition on Ag-Z5 and CLD-Ag-Z5 could be due to the loss of silver during the catalyst preparation process.

XPS measurement was employed to detect the Ag atom on the external surface of Ag-incorporated HZSM-5 zeolites. In **Table 4.2**, the surface Ag-composition on CLD-Ag-Z5 (2.20 wt%) was higher than that of Ag-Z5 (1.68 wt%), confirming the existence as well as enrichment of silver on the external surface of CLD-Ag-Z5. It was consistent with the results of TEM analysis. The undetected amount of surface Ag-composition on S-CLD-Ag-Z5 could be due to the interaction between SO_4^{2-} group and silver oxide at the surface of S-CLD-Ag-Z5, leading low amount of Ag-composition in S-CLD-Ag-Z5.

Table 4.2 The Ag-composition of prepared ZSM-5 catalysts

Catalysts	Ag composition (% wt)		
	Theory	Bulk*	Surface**
Ag-Z5	1.0	0.703	1.68
CLD-Ag-Z5	1.0	0.822	2.20

* Analyzed by XRF.

** Analyzed by XPS.

States of Ag species on the external surface were examined by XPS measurement. Although the depth of Ag species detectable by XPS is limited (<10 nm), it provided a rough picture of the nature of part of Ag introduced into the ZSM-5. As shown in **Figure 4.4 (a)**, five existence states of Ag species over Ag-Z5 catalyst can be differentiated via deconvolution of $Ag_{3d5/2}$ profiles. The binding energies were 368.2 eV, 368.7 eV, 369.3 eV, 369.5 eV, and 370.4 eV, belonging to AgO , Ag_2O , Ag_n^0 , Ag^+ , and Ag_n^{d+} , respectively. In **Figure 4.4 (b)**, the binding energies of $Ag_{3d5/2}$ over CLD-Ag-Z5 were 366.3 eV, 367.1 eV, 367.5 eV, 368.9 eV, and 369.8 eV, belonging to AgO , Ag_2O , Ag_n^0 , Ag^+ and Ag_n^{d+} respectively. The shift of binding energies of $Ag_{3d5/2}$ over Ag-Z5 and CLD-Ag-Z5 was in the standard binding energy range of $Ag_{3d5/2}$ spectra (Moulder and Chastain, 1992). Compared with Ag-Z5, the binding energies of $Ag_{3d5/2}$ over CLD-Ag-Z5 shifted to a lower value compared to that of Ag-Z5. It can be deduced that the CLD strategy introduced Ag atoms concentrated on to the external surface of ZSM-5 zeolites giving low binding energy, while the impregnation method helped Ag atom interact with or enter into the framework of ZSM-5 zeolites leading to the higher binding energies (Hou *et al.*, 2019).

Several Ag species such as Ag^+ (isolated silver ions in the zeolites), Ag_n^{d+} (silver species absorbed on framework oxygen), Ag_n^0 (metallic silver particles) and Ag_2O in zeolite can promote the cracking activity and act as new Lewis acid sites. These Lewis acid sites created by transition metals would promote the catalytic cracking activity by enhancing the dehydrogenation reactions of hydrocarbons (Qiu *et al.*, 2014).

Moreover, most of the Ag species in Ag-Z5 and CLD-Ag-Z5 were Ag_n^0 , AgO and Ag_2O . For sulfated catalyst, the two oxygen atoms of SO_4^{2-} group bond with the metal atoms of metal oxide at the catalyst surface (Hu *et al.*, 2015). Therefore, the silver oxide species were occupied by the SO_4^{2-} groups leading the lower Ag species in S-CLD-Ag-Z5. Thus, the surface Ag-composition of S-CLD-Ag-Z5 was not detected by XPS which was lower than detection limit for XPS.

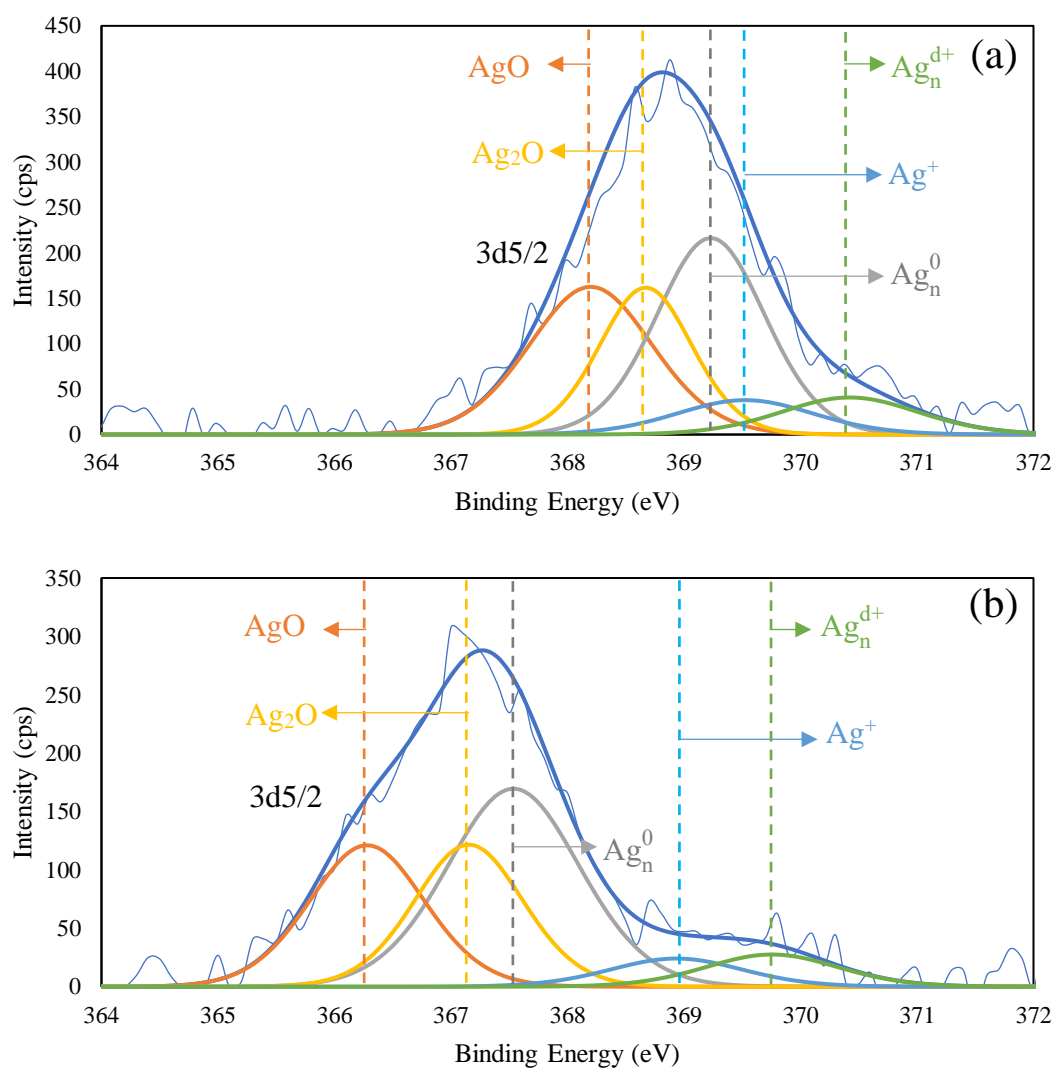


Figure 4.4 Ag_{3d5/2} XPS spectra of (a) Ag-Z5 and (b) CLD-Ag-Z5.

4.2 Catalytic Activity Testing

To investigate the effects of silver distribution on the catalytic activities of HZSM-5 and modified HZSM-5 catalysts, *n*-pentane catalytic cracking was performed at 550 °C under atmospheric pressure with *n*-pentane WHSV of 5 h⁻¹ and maintained the reaction for 6 h. All the results are considered at time on stream (TOS) of 4 h.

Figure 4.5 exhibits the conversion of *n*-pentane, ethylene yield, propylene yield and light olefins yield from HZSM-5 and modified HZSM-5 catalysts. It was found that the obtained conversion from HZSM-5 and modified HZSM-5 catalysts ranged from 88.89% to 93.13%. The conversion of *n*-pentane and ethylene yield were increased after Ag-incorporation in HZSM-5 zeolites, indicating that Ag-incorporation was beneficial to promote catalytic activity as well as ethylene production and achieve higher light olefins yield in *n*-pentane catalytic cracking. Compared with P-Z5, the modified HZSM-5 catalysts exhibited a higher conversion and light olefins yield. Ag-Z5, CLD-Ag-Z5 and S-CLD-Ag-Z5 exhibited an *n*-pentane conversion of 93.13%, 89.99% and 91.32%, respectively, which were higher than that of P-Z5 (88.89%). The yield of ethylene was 18.88% over P-Z5, and it was increased to 23.08%, 24.20% and 25.60% over Ag-Z5, CLD-Ag-Z5 and S-CLD-Ag-Z5, respectively.

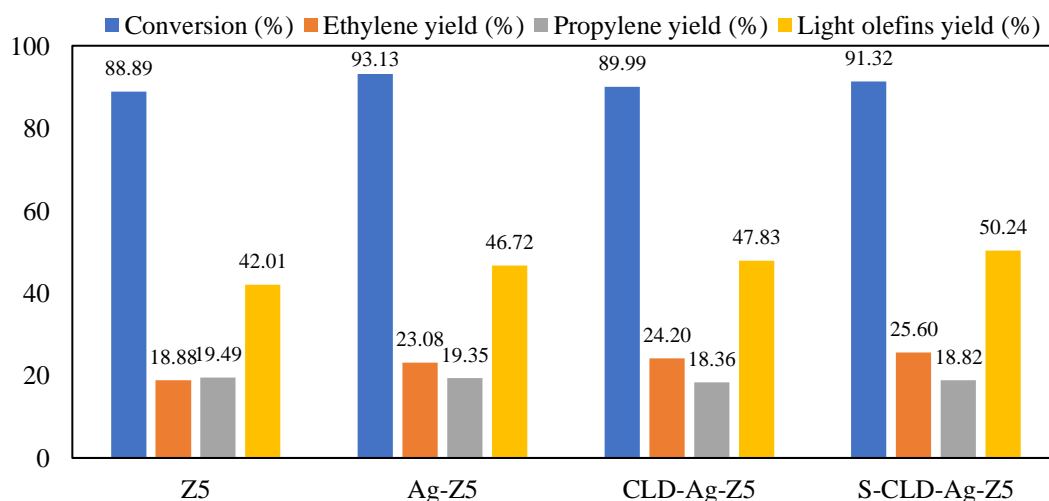


Figure 4.5 Conversion of *n*-pentane, ethylene yield, propylene yield and light olefins yield from P-Z5, Ag-Z5, CLD-Ag-Z5 and S-CLD-Ag-Z5 at 550 °C.

The results of light olefins and paraffins yield from P-Z5, Ag-Z5, CLD-Ag-Z5 and S-CLD-Ag-Z5 at 550 °C are presented in **Figure 4.6**. Compared with P-Z5, the modified HZSM-5 catalysts increased light olefins yield while decreased paraffins yield, confirming Ag-incorporation promoted light olefins production in *n*-pentane catalytic cracking.

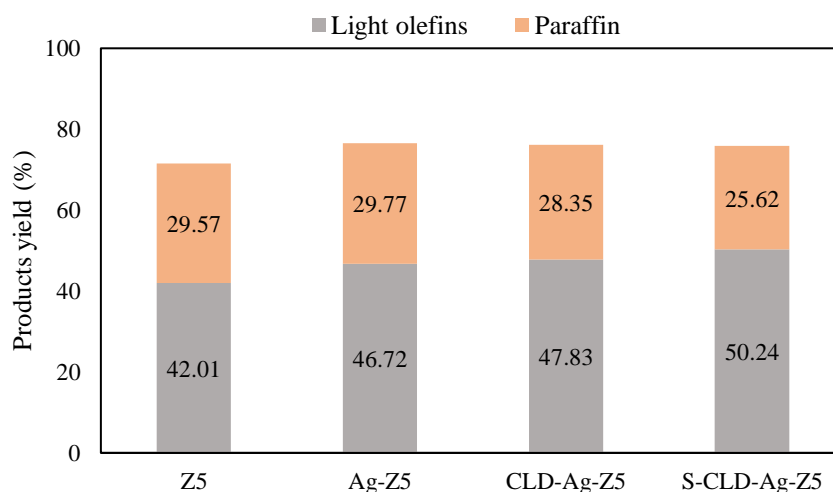


Figure 4.6 Products yield of light olefins and paraffins from P-Z5, Ag-Z5, CLD-Ag-Z5 and S-CLD-Ag-Z5 at 550 °C.

The product distribution for *n*-pentane catalytic cracking over ZSM-5 zeolites at 550 °C including methane, ethane, ethylene, propylene, propane, butane, butylenes, and C₅⁺ products are presented in **Figure 4.7**. Ethylene, propylene, butylenes, ethane, propane and butane occupied the majority (> 74%) in the final product. Compared with P-Z5, Ag-Z5, CLD-Ag-Z5, and S-CLD-Ag-Z5 exhibited lower the selectivity to propylene and ethane with higher selectivity to ethylene. The monomolecular protolytic cracking of *n*-pentane over the Brønsted acid sites generating ethane with carbenium ions (route M3) was most favored by energetic demand (Hou, Qiu, Yuan, Zhang, *et al.*, 2017). Moreover, Ag-incorporation significantly enhanced C-H bond breaking and alkenes formation giving a higher ethylene selectivity. In addition, S-CLD-Ag-Z5 further increased the selectivity to ethylene, indicating that sulfation method remarkably enhanced the dehydrogenation reactions in comparison to CLD-Ag-Z5.

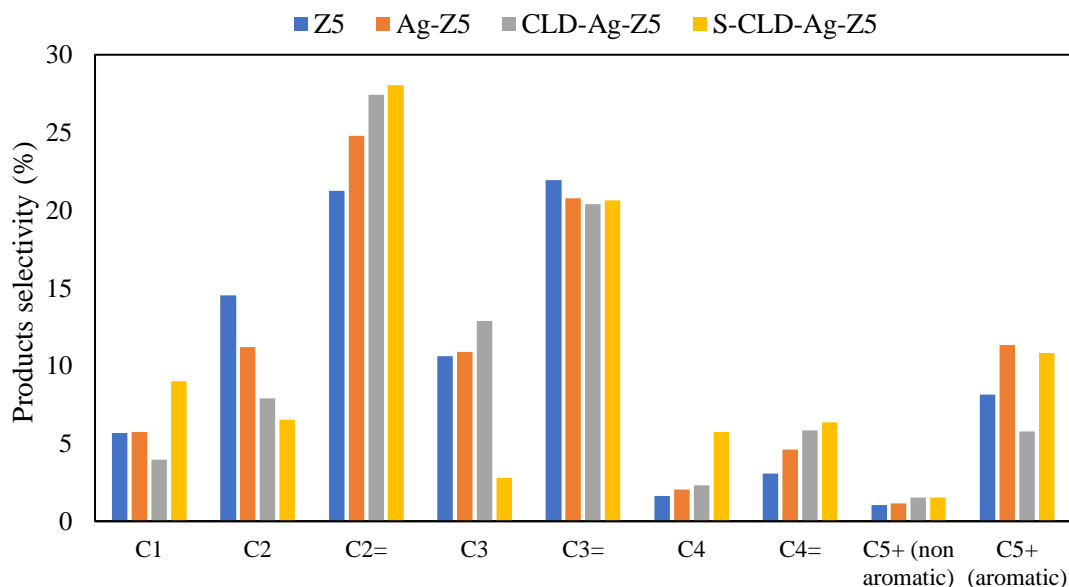


Figure 4.7 Products distribution from P-Z5, Ag-Z5, CLD-Ag-Z5 and S-CLD-Ag-Z5 at 550 °C.

As shown in **Figure 4.8**, Ag-Z5, CLD-Ag-Z5 and S-CLD-Ag-Z5 gave a higher ethylene selectivity than that of P-Z5. Ethylene selectivity obtained over Ag-Z5, CLD-Ag-Z5 and S-CLD-Ag-Z5 were 24.78%, 26.89%, and 28.03%, respectively, which were higher than that of P-Z5 (21.24%). Selectivity to propylene over Ag-Z5, CLD-Ag-Z5 and S-CLD-Ag-Z5 were slightly lower than that of P-Z5.

For the propylene to ethylene ratio of HZSM-5 and modified HZSM-5 catalysts, The HZSM-5 and modified HZSM-5 catalysts was consistent with the results of ethylene selectivity and propylene selectivity that the propylene selectivity is lower than ethylene selectivity. In addition, the S-CLD-Ag-Z5 catalyst exhibited the lowest propylene to ethylene ratio of 0.74. It can be deduced that the S-CLD-Ag-Z5 catalyst enhanced ethylene production in *n*-pentane catalytic cracking.



1518776057

CD IThesis 6271012063 thesis / rev: 09092564 02:41:52 / seq: 101

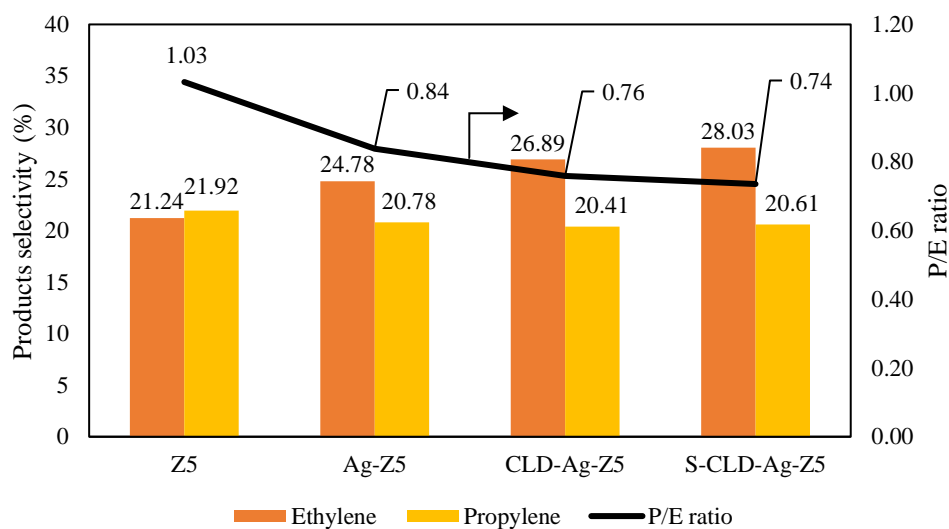


Figure 4.8 Ethylene selectivity, propylene selectivity and propylene to ethylene ratio from P-Z5, Ag-Z5, CLD-Ag-Z5 and S-CLD-Ag-Z5 at 550 °C.

It can be concluded that Ag-incorporation significantly promoted the catalytic activity in *n*-pentane catalytic cracking at 550 °C. It was probably due to the enhanced formation of alkenes via dehydrogenation cracking over Ag sites, which was easily protonated by Brønsted acid sites and accelerated the conversion of alkanes (Hou, Qiu, Zhang, *et al.*, 2017). Ag sites interacted with hydrogen atoms of alkanes, enhance the dissociation of C-H bond, and promote the formation of hydrogen and olefins.

Although the promotion of Ag-Z5, CLD-Ag-Z5 and S-CLD-Ag-Z5 on *n*-pentane catalytic cracking was probably attributed to the enhancement of dehydrogenation reactions, CLD-Ag-Z5 behaved in a different way in comparison to Ag-Z5. The promotion caused by Ag-CLD modification can be attributed to the porous silver overlayer on the external surface of CLD-Ag-Z5. CLD strategy decreased Brønsted acid sites by the selective passivation and increased Lewis acid sites by dehydroxylation of Brønsted acid sites at high temperature leading to the change on acid properties of CLD-Ag-Z5 (Hou *et al.*, 2016). Therefore, the modified external surface can improve the reorientation of *n*-pentane molecules in the surface layer and guiding them into the micropore system, and thus promote the interphase mass transfer which led to a higher *n*-pentane concentration within the channels. Thus, CLD-Ag-Z5 remarkably promoted the catalytic activity in *n*-pentane catalytic cracking compared to



1518776057

Ag-Z5. While the Ag-incorporation of ZSM-5 zeolites by impregnation method enhanced the interaction between *n*-pentane molecules and Brønsted acid sites or carbenium ions, which promoted catalytic cracking.

For S-CLD-Ag-Z5 catalyst, the further promotion of the S-CLD-Ag-Z5 catalysts in *n*-pentane cracking can be attributed to the introduction of SO_4^{2-} group interacting with the silver oxide at the surface. The electron withdrawing S=O covalent bond induces metal atoms to manifest electron-deficiency, forming Lewis acid sites. The acidic proton derived from the surface hydroxyl group of metal oxides linked to the Lewis acid site can be easily released to introduce a Brønsted acid site (Hu *et al.*, 2015). Therefore, the new electron distribution on the surface would make a difference on acid properties of S-CLD-Ag-Z5. The sulfate phase promoted the paraffin saturation adsorption. Moreover, the sulfate phase also significantly enhanced the diffusion process of the *n*-pentane in the S-CLD-Ag-Z5 catalyst, accelerated the sorption process for the gas-phase *n*-pentane molecules into the micropores and thus increased the *n*-pentane concentration in the micropores of the catalyst (Hou, Qiu, Yuan, Zhang, *et al.*, 2017). Thus, the excellent catalytic activity for *n*-pentane catalytic cracking was achieved over the S-CLD-Ag-Z5 catalysts.

4.3 Catalytic Stability

The catalytic stability was performed at 550 °C under atmospheric pressure with *n*-pentane WHSV of 5 h⁻¹ and maintained the reaction for 6 h. The obtained conversion and light olefins selectivity, ethylene selectivity and propylene selectivity as a function of time on stream (TOS) are shown in **Figures 4.9, 4.10, 4.11** and **4.12**, respectively.

The HZSM-5 and modified HZSM-5 catalysts exhibited high conversion ranging from 86.05% to 95.99% and maintained the good stability even after a long time. Compared with HZSM-5 catalyst, the modified HZSM-5 catalysts provided higher stability. It can be concluded that the catalyst modification can improve catalytic stability in *n*-pentane catalytic cracking.

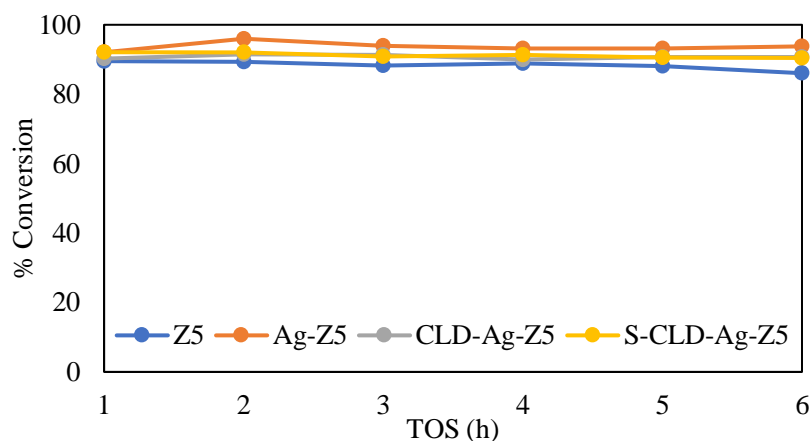


Figure 4.9 Conversion of *n*-pentane from P-Z5, Ag-Z5, CLD-Ag-Z5 and S-CLD-Ag-Z5 at 550 °C as a function of time on stream (TOS).

The results of light olefins selectivity, ethylene selectivity and propylene selectivity from HZSM-5 and modified HZSM-5 catalysts are shown in **Figures 4.10**, **4.11** and **4.12**. S-CLD-Ag-Z5 catalyst provided the highest light olefins selectivity, ethylene selectivity in comparison to the parent HZSM-5 and other modified HZSM-5 catalysts. Moreover, S-CLD-Ag-Z5 also maintained a good stability after 6 h. Compared with HZSM-5, the modified HZSM-5 catalysts exhibited lower propylene selectivity. It can be concluded that the catalyst modification cannot only improve catalytic stability but also maintain a good catalytic activity after a long time of reaction.

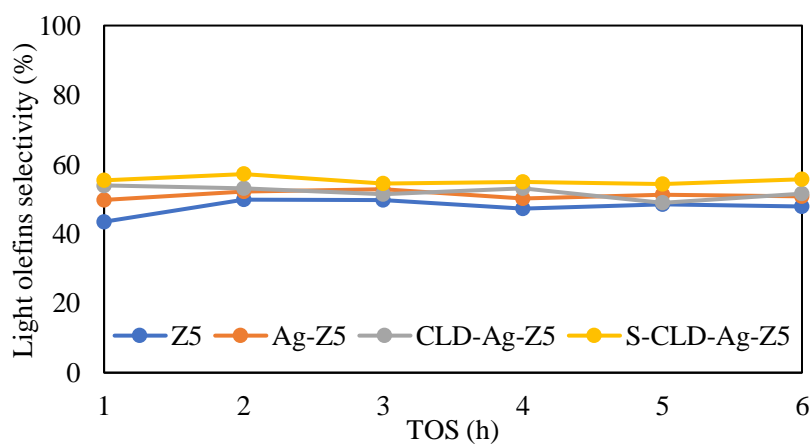


Figure 4.10 Light olefins selectivity from P-Z5, Ag-Z5, CLD-Ag-Z5 and S-CLD-Ag-Z5 at 550 °C as a function of time on stream (TOS).

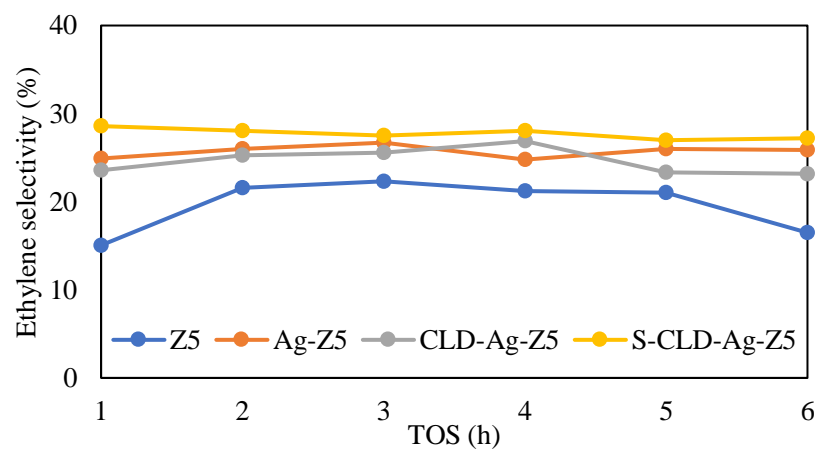


Figure 4.11 Ethylene selectivity from P-Z5, Ag-Z5, CLD-Ag-Z5 and S-CLD-Ag-Z5 at 550 °C as a function of time on stream (TOS).

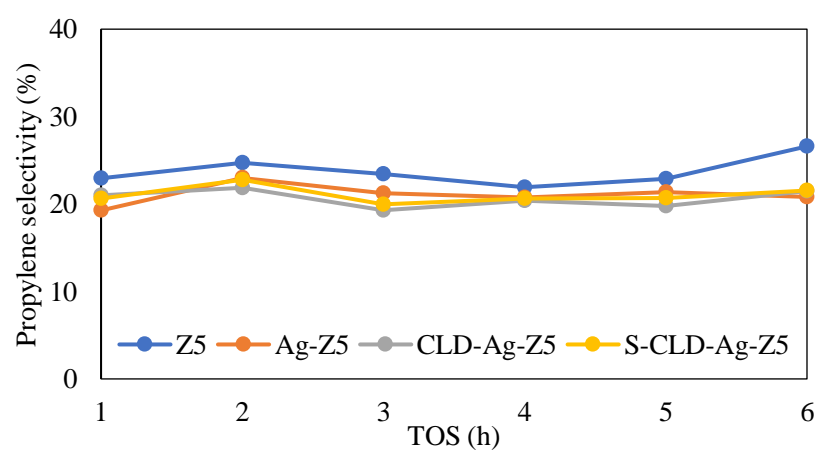


Figure 4.12 Propylene selectivity from P-Z5, Ag-Z5, CLD-Ag-Z5 and S-CLD-Ag-Z5 at 550 °C as a function of time on stream (TOS).

CHAPTER 5

CONCLUSION AND RECOMMENDATIONS

5.1 Conclusion

To study the effects of Ag-incorporation on the catalytic performance of ZSM-5 zeolites, Ag-incorporation was carried out via the impregnation and chemical liquid deposition (CLD) and sulfation methods to evaluate light olefins production in *n*-pentane catalytic cracking. The catalyst characterizations including XRD, TEM, XRF, and XPS, confirmed that the characteristic ZSM-5 zeolite structure was well preserved after the Ag-incorporation by impregnation, CLD, and sulfation methods. TEM images provided the rough phase of Ag-incorporated HZSM-5 zeolites which can be attributed to the silver concentrating on external surface. TEM image also showed its rough surface of S-CLD-Ag-Z5 confirming the sulfate phase was generated on the surface. In addition, the surface Ag-composition on CLD-Ag-Z5 was higher than that of Ag-Z5, confirming the existence as well as enrichment of silver on the external surface of CLD-Ag-Z5. The N₂ adsorption and desorption results suggested that the silver overlayer generated by the CLD and sulfation methods was probably mesoporous phase and expanded the external surface of CLD-Ag-Z5 and S-CLD-Ag-Z5.

In *n*-pentane catalytic cracking at 550 °C, Ag-incorporation promoted the conversion and light olefins yield. Moreover, silver also increased the selectivity to ethylene, while decreased the selectivity to propylene and ethane in comparison to P-Z5. It was probably due to the enhanced formation of alkenes via dehydrogenation cracking over Ag sites. The catalytic stability was performed at 550 °C and maintained the reaction for 6 h. Ag-Z5, CLD-Ag-Z5 and S-CLD-Ag-Z5 were more efficient to maintain catalytic activity in *n*-pentane catalytic cracking in comparison to P-Z5.

As expected, S-CLD-Ag-Z5 exhibited the highest light olefins production and maintain a good stability in *n*-pentane catalytic cracking. The promotion of S-CLD-Ag-Z5 was attributed to promote the *n*-pentane saturation adsorption at the external surface and enhance sorption process of *n*-pentane molecules into the micropores of ZSM-5 zeolite.



1518776057

CD IThesis 6271012063 thesis / rev: 09092564 02:41:52 / seq: 101

5.2 Recommendations

The researcher recommends that temperature programmed reduction (H₂-TPR), temperature programmed desorption of ammonia (NH₃-TPD), Infrared spectroscopy of pyridine and 2,4,6-trimethylpyridine adsorption (Py-IR and TMPy-IR) are necessary to investigate the acid properties of HZSM-5 and modified HZSM-5 catalysts to obtain more understandable information.

Transmission electron microscope (TEM) with an energy dispersive X-ray (EDX) point scan analysis and X-ray photoelectron spectroscopy (XPS) with narrow scan mode are necessary to determine the amount of sulfur composition and clarify the existence of SO₄²⁻ group at the external surface of S-CLD-Ag-Z5.

For catalytic stability, temperature programmed oxidation (TPO) and CHNS elemental analyzer are necessary to determine the amount of coke and carbon of spent catalysts to confirm the catalytic stability results of HZSM-5 and modified HZSM-5 catalysts.

APPENDICES

Appendix A Graphical Abstract

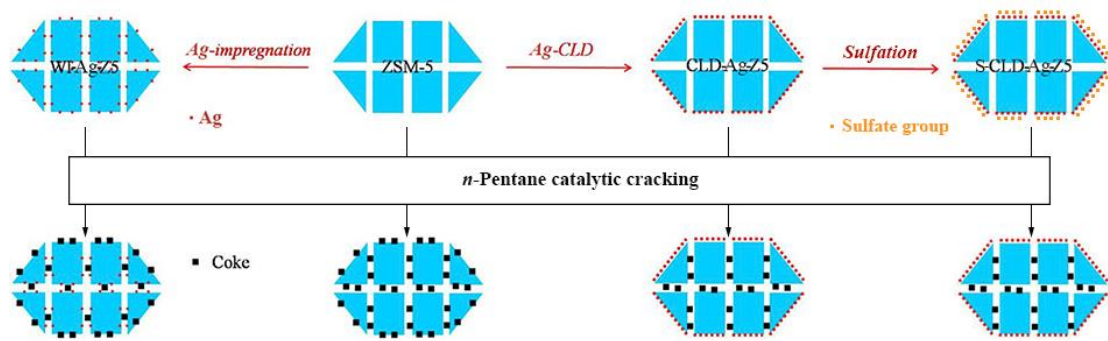


Figure A1 Graphical Abstract.

Appendix B Hydrocarbon Gas Standard

Table B1 Retention times of the hydrocarbon gas standard

Hydrocarbon Species	Retention Time (min)
Methane	1.099
Ethane	1.366
Ethylene	1.989
Propane	2.995
Propylene	5.894
Isobutane	6.559
Butane	7.034
Propadiene	7.959
Acetylene	8.931
trans-2-Butene	10.203
Butene-1	10.598
Isobutylene	11.168
cis-2-Butene	11.586
Isopentane	12.014
<i>n</i> -Pentane	12.675



1518776057

CU IThesis 6271012063 thesis / recv: 09092564 02:41:52 / seq: 101

Appendix C GC-FID Chromatogram Results

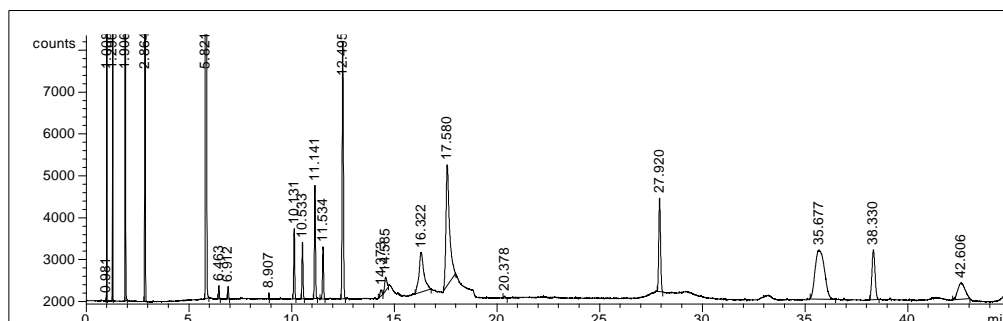


Figure C1 GC-FID Chromatogram of HZSM-5 catalyst at TOS 1 h.

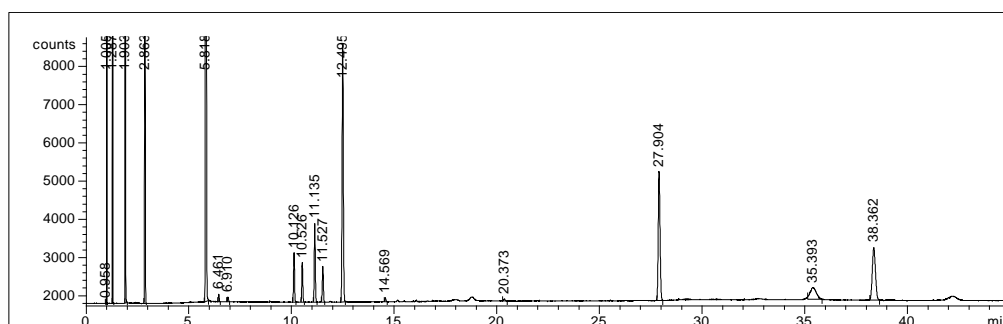


Figure C2 GC-FID Chromatogram of HZSM-5 catalyst at TOS 2 h.

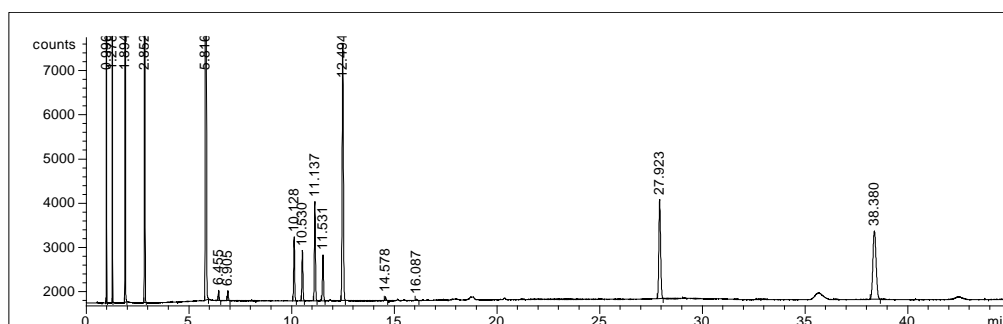


Figure C3 GC-FID Chromatogram of HZSM-5 catalyst at TOS 3 h.

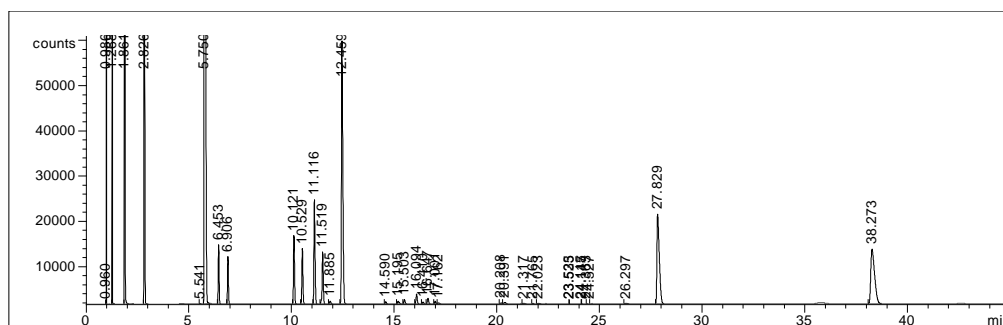


Figure C4 GC-FID Chromatogram of HZSM-5 catalyst at TOS 4 h.

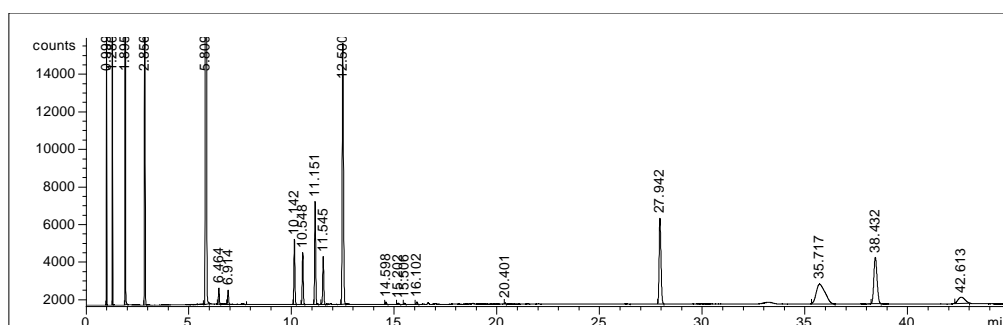


Figure C5 GC-FID Chromatogram of HZSM-5 catalyst at TOS 5 h.

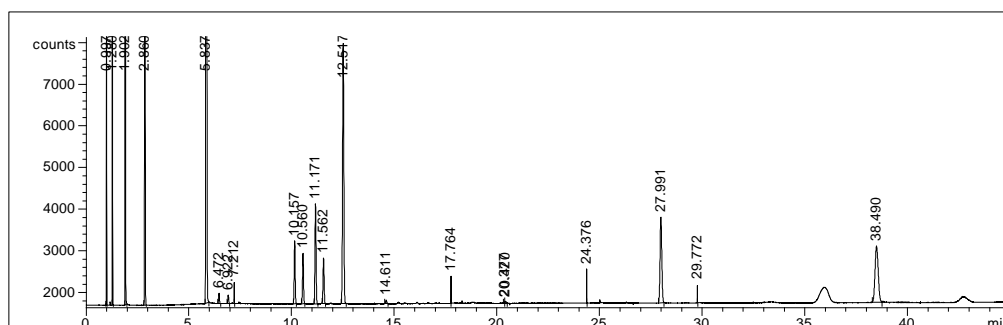


Figure C6 GC-FID Chromatogram of HZSM-5 catalyst at TOS 6 h.

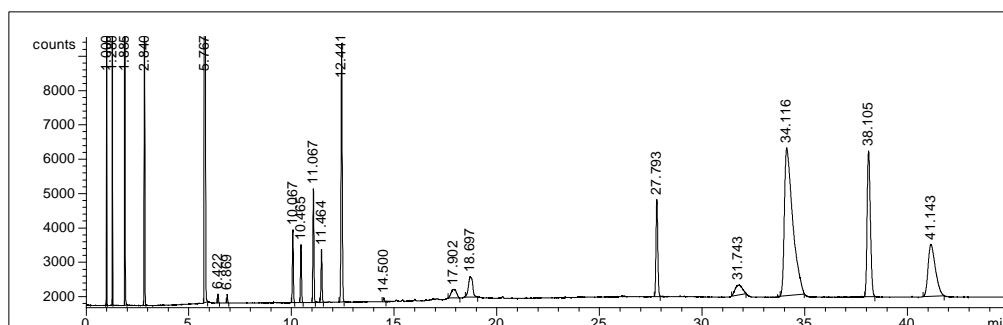


Figure C7 GC-FID Chromatogram of Ag-Z5 catalyst at TOS 1 h.



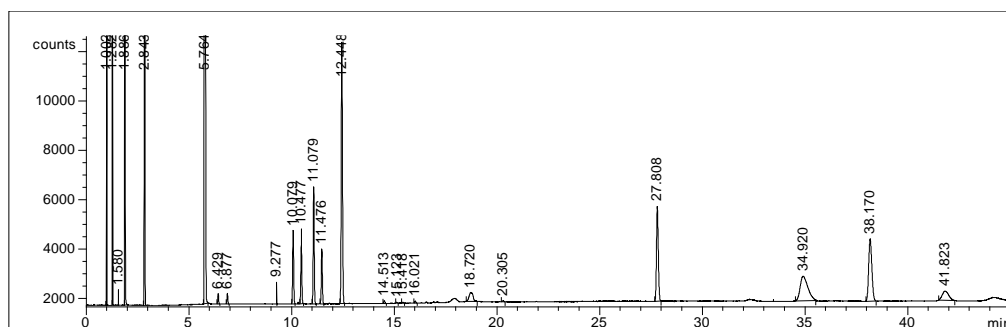


Figure C8 GC-FID Chromatogram of Ag-Z5 catalyst at TOS 2 h.

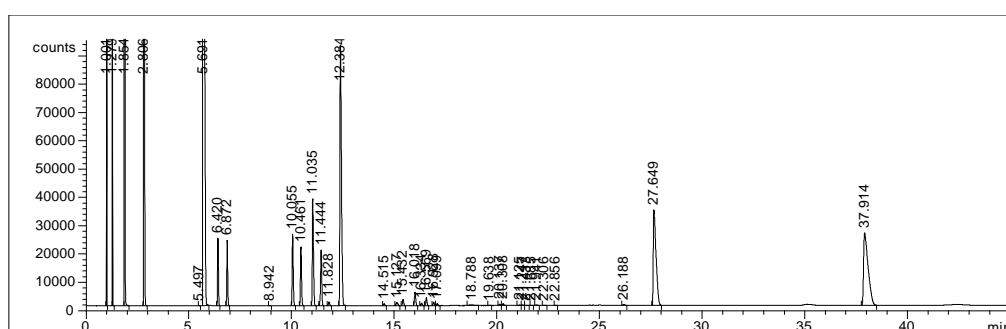


Figure C9 GC-FID Chromatogram of Ag-Z5 catalyst at TOS 3 h.

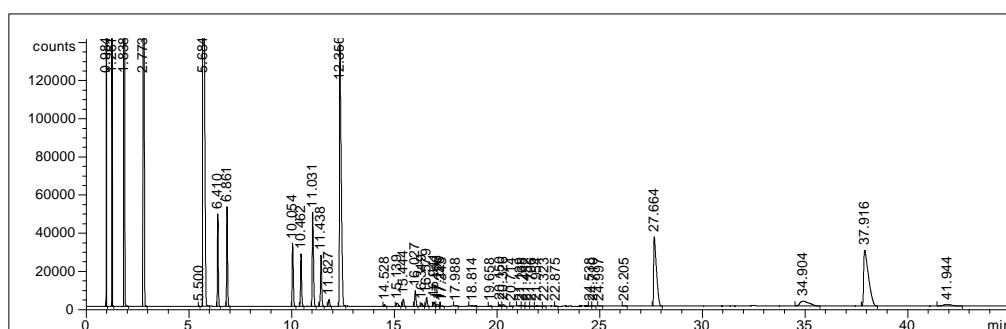


Figure C10 GC-FID Chromatogram of Ag-Z5 catalyst at TOS 4 h.

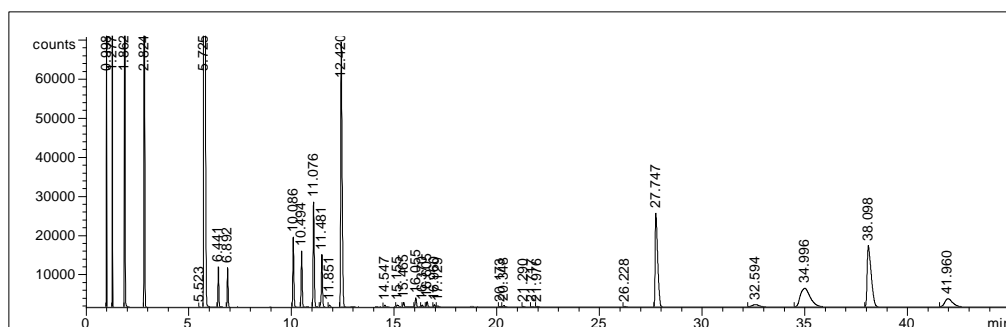


Figure C11 GC-FID Chromatogram of Ag-Z5 catalyst at TOS 5 h.

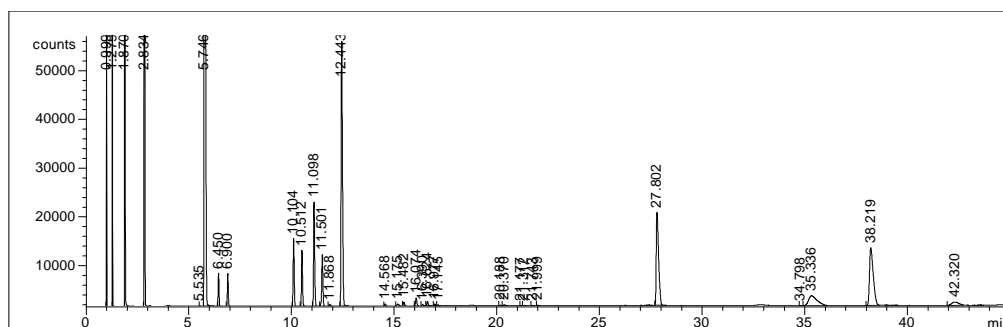


Figure C12 GC-FID Chromatogram of Ag-Z5 catalyst at TOS 6 h.

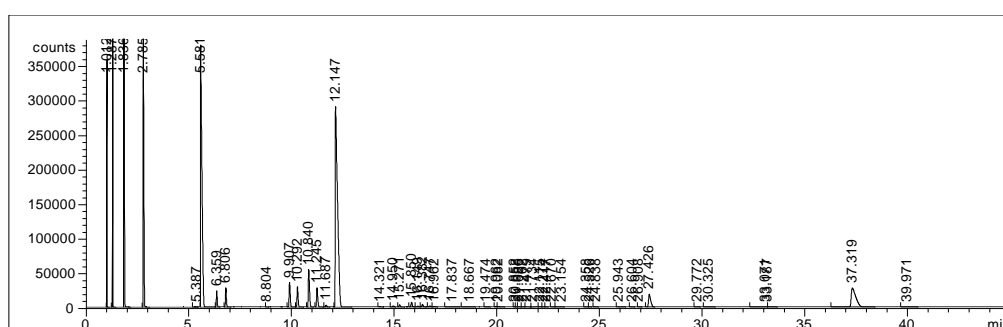


Figure C13 GC-FID Chromatogram of CLD-Ag-Z5 catalyst at TOS 1 h.

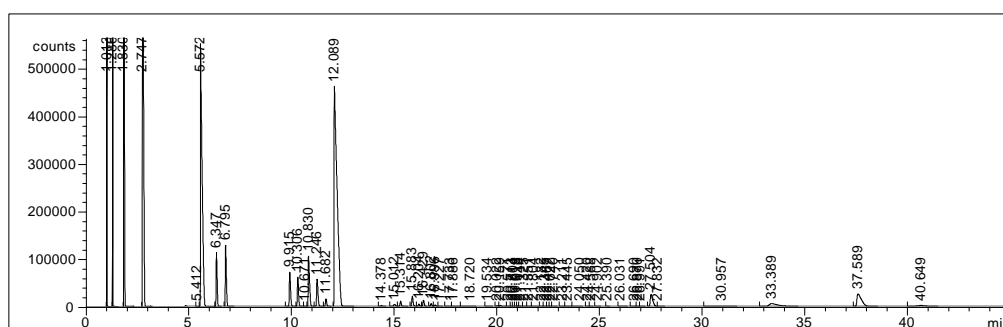


Figure C14 GC-FID Chromatogram of CLD-Ag-Z5 catalyst at TOS 2 h.

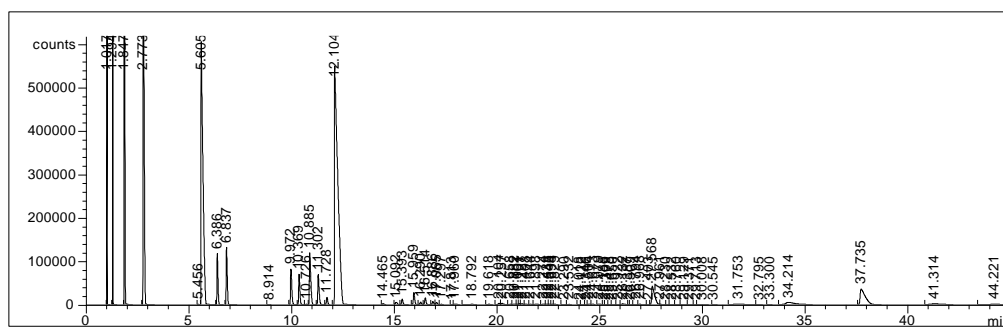


Figure C15 GC-FID Chromatogram of CLD-Ag-Z5 catalyst at TOS 3 h.

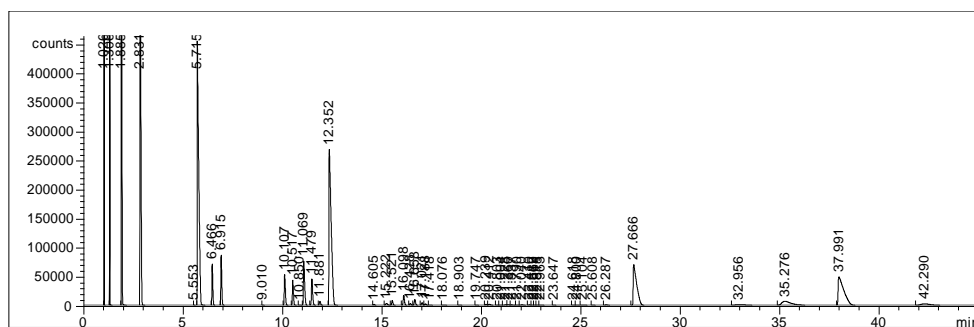


Figure C20 GC-FID Chromatogram of S-CLD-Ag-Z5 catalyst at TOS 2 h.

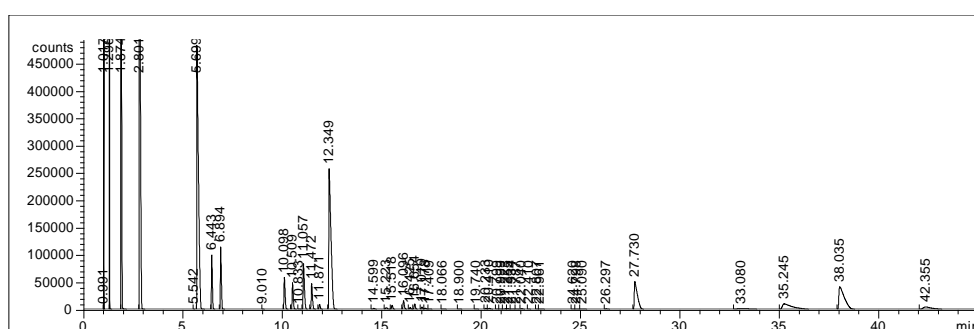


Figure C21 GC-FID Chromatogram of S-CLD-Ag-Z5 catalyst at TOS 3 h.

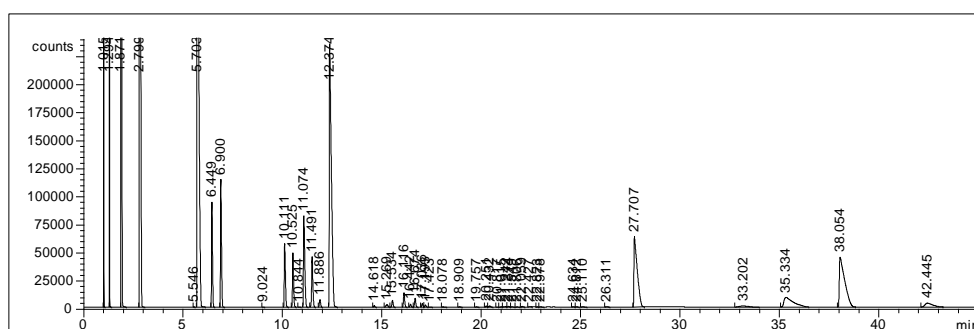


Figure C22 GC-FID Chromatogram of S-CLD-Ag-Z5 catalyst at TOS 4 h.

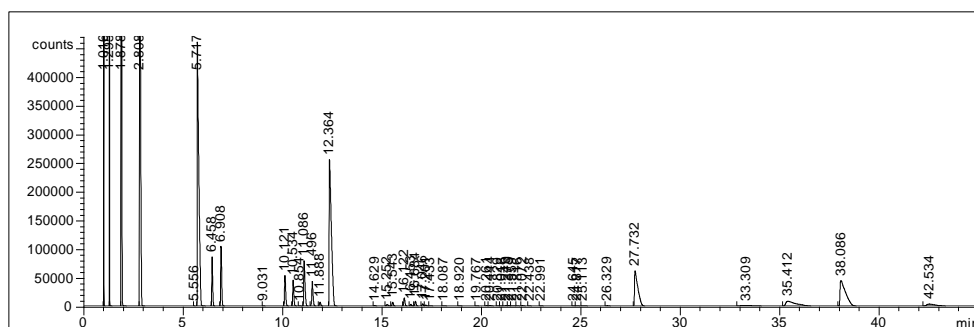


Figure C23 GC-FID Chromatogram of S-CLD-Ag-Z5 catalyst at TOS 5 h.

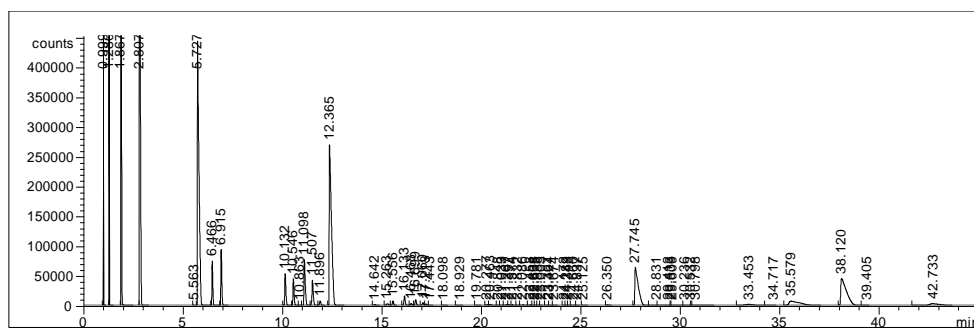


Figure C24 GC-FID Chromatogram of S-CLD-Ag-Z5 catalyst at TOS 6 h.



1518776057

CU IThesis 6271012063 thesis / recv: 09092564 02:41:52 / seq: 101

Appendix D Calculation of Activity Testing

Calculation of *n*-pentane feed flow rate at $WHSV = 5 \text{ h}^{-1}$

Amount of HZSM-5 catalyst = 2.00 g

$$WHSV = \frac{\text{Flow rate } \left(\frac{\text{g}}{\text{h}}\right)}{\text{Weight of catalyst (g)}}$$

$$5 \text{ h}^{-1} = \frac{\text{Flow rate } \left(\frac{\text{g}}{\text{h}}\right)}{2.00 \text{ g}}$$

$$\text{Flow rate} = 10.00 \text{ g/h}$$

According to *n*-pentane density which is equal to 0.626 g/mL at 20 °C, 1 atm

$$\text{Flow rate} = \frac{10.00 \text{ g/h}}{0.626 \text{ g/mL}} = 15.97 \text{ mL/h}$$



151876057

REFERENCES

- Amghizar, I., Vandewalle, L.A., Van Geem, K.M., and Marin, G.B. (2017). New trends in olefin production. Engineering, 3(2), 171-178.
- Diao, Z., Wang, L., Zhang, X., and Liu, G. (2015). Catalytic cracking of supercritical n-dodecane over meso-HZSM-5@Al-MCM-41 zeolites. Chemical Engineering Science, 135, 452-460.
- Hou, X., Qiu, Y., Yuan, E., Li, F., Li, Z., Ji, S., Yang, Z., Liu, G., and Zhang, X. (2017). Promotion on light olefins production through modulating the reaction pathways for n-pentane catalytic cracking over ZSM-5 based catalysts. Applied Catalysis A: General, 543, 51-60.
- Hou, X., Qiu, Y., Yuan, E., Zhang, X., and Liu, G. (2017). SO₂/TiO₂ promotion on HZSM-5 for catalytic cracking of paraffin. Applied Catalysis A: General, 537, 12-23.
- Hou, X., Qiu, Y., Zhang, X., and Liu, G. (2016). Catalytic cracking of n-pentane over CLD modified HZSM-5 zeolites. RSC advances, 6(59), 54580-54588.
- Hou, X., Qiu, Y., Zhang, X., and Liu, G. (2017). Analysis of reaction pathways for n-pentane cracking over zeolites to produce light olefins. Chemical Engineering Journal, 307, 372-381.
- Hou, X., Zhu, W., Tian, Y., Qiu, Y., Diao, Z., Feng, F., Zhang, X., and Liu, G. (2019). Superiority of ZrO₂ surface enrichment on ZSM-5 zeolites in n-pentane catalytic cracking to produce light olefins. Microporous and Mesoporous Materials, 276, 41-51.
- Hu, Y., Guo, B., Fu, Y., Ren, Y., Tang, G., Chen, X., Yue, B., and He, H. (2015). Facet-dependent acidic and catalytic properties of sulfated titania solid superacids. Chemical Communications, 51(75), 14219-14222.
- Moulder, J.F., and Chastain, J. (1992). Handbook of X-ray Photoelectron Spectroscopy: A Reference Book of Standard Spectra for Identification and Interpretation of XPS Data, Physical Electronics Division, Perkin-Elmer Corporation.
- Qiu, Y., Zhao, G., Liu, G., Wang, L., and Zhang, X. (2014). Catalytic Cracking of Supercritical n-Dodecane over Wall-Coated Nano-Ag/HZSM-5 Zeolites. Industrial & Engineering Chemistry Research, 53(47), 18104-18111.

- Vasudev Pralhad Haribal, Y.C., Luke Neal, Fanxing Li (2018). Intensification of Ethylene Production from Naphtha via a Redox Oxy-Cracking Scheme: Process Simulations and Analysis. Engineering, 4(5), 714-721.
- Yaripour, F., Shariatnia, Z., Sahebdehfar, S., and Irandoukht, A. (2015). Conventional hydrothermal synthesis of nanostructured H-ZSM-5 catalysts using various templates for light olefins production from methanol. Journal of Natural Gas Science and Engineering, 22, 260-269.
- Yu, H., Wang, X.-q., and Long, Y.-c. (2006). Synthesis of b-axis oriented high silica MFI type zeolite crystals introduced with co-template role. Microporous and Mesoporous Materials, 95(1-3), 234-240.



1518776057

CU IThesis 6271012063 thesis / recv: 09092564 02:41:52 / seq: 101

VITA

NAME	Warisara Angguravanich
DATE OF BIRTH	10 May 1997
PLACE OF BIRTH	Bangkok
INSTITUTIONS ATTENDED	2019 - 2020 Master of Science in Petrochemical Technology, The Petroleum and Petrochemical College, Chulalongkorn University, Bangkok, Thailand. 2015 - 2018 Bachelor of Engineering in Petrochemicals and Polymeric Materials, Faculty of Engineering and Industrial Technology, Silpakorn University, Nakorn Pathom, Thailand
HOME ADDRESS	497, Soi Thian-talay 9/1, Bangkhunthian-chaytalay Rd., Samae Dam, Bangkhunthian, Bangkok, 10150.



1518776057

CU ThesIs 6271012063 thesis / recv: 09092564 02:41:52 / seq: 101